The Behaviour of Nanoclay Modified Asphalt Binders and Mixtures

by

Liniker Lettiere Ferreira Monteiro

A thesis submitted in partial fulfillment of the requirements for the degree of

Master of Science

in

Civil (Cross-disciplinary)

Department of Civil and Environmental Engineering
University of Alberta

Abstract

Asphalt pavement is subject to stresses induced by heavy traffic loading and thermal variations during its service life. Nowadays, increasing the permissible axle loads along with the impact of climate change have caused premature failure in the flexible pavement. Enhancing the properties of asphalt binders can reduce these distresses. Among the available options, finding a cost-effective alternative for improving the used binders is a challenge to overcome. Asphalt binder modification using nano-size materials has attracted attentions in recent years. Based on this study, nanoclays can improve the properties of asphalt binders, increase the resistance of asphalt to ageing, cracking and rutting, and extend the pavement's service life cycle. The objectives of this work were to investigate the rheological and mechanical properties of nanoclay modified asphalt binders and mixtures. The behaviour of a PG 64-28 asphalt binder modified with 2% and 4% concentration of two organo-montmorillonites was studied. Furthermore, the impact of using nanoclays was investigated in asphalt mixtures' performance. The nanoclays were mixed with the asphalt using a high shear mixer, and their dispersions were analyzed by employing a Scanning Electron Microscope (SEM) device. A SARA test was conducted on the modified and unmodified binders to examine the fraction composition of saturates, asphaltenes, resins and aromatics before and after the addition of nanoclays. Also, the neat binder and the nanoclay modified binders were subjected to short-term ageing using a rolling thin-film oven (RTFO) and long-term aged using a pressure ageing vessel (PAV). The following rheological properties of the asphalt binders were investigated: (1) High-temperature performance grading of unaged samples using a dynamic shear rheometer (DSR), (2) High-temperature performance grading of RTFO-aged samples using a DSR, (3) Intermediate temperature grading of PAV-aged samples using a DSR, (5) Low-temperature performance grading using a bending beam rheometer (BBR), (4) Two-piece healing test using a DSR, (6) Frequency-Sweep tests using a DSR, (7) Mixing and Compaction temperatures using a rotational viscometer, and (8) Mixing and compaction

temperatures of modified asphalt binders using a DSR. Additionally, the mechanical properties of the asphalt mixtures that were analyzed are as follows: (1) Flow and Stability and stability test, (2) Bulk specific gravity test, (3) Theoretical maximum specific gravity on loose mixtures, (4) Fatigue and healing behaviour using a four-point bending test and (5) Dynamic Modulus test on Superpave samples.

The results obtained from the high-temperature grading showed that the addition of 4% organo-montmorillonites increases the high-temperature grade from 64 to 70. Also, no change was observed in the low-temperature performance of the modified samples. The two-piece healing test showed promising results for nano-modified samples, with significant improvements in the initial healing proportional to the concentration of nanoclays in the binder. The Frequency-sweep analysis, utilizing a master curve, showed an improvement in ageing resistance by adding Montmorillonites. Furthermore, the SARA test results indicated that the nanoclay modified mixtures were storage stable. The asphalt mixture samples demonstrated, by repeated flexural bending using a four-point bending apparatus, increased stiffness and life cycles of the organo-montmorillonite modified asphalt mixtures.

Preface

This thesis is an original work by Liniker Lettiere Ferreira Monteiro under the supervision of Dr. Leila Hashemian. Chapters 1 and 2, which are based on a literature review and introduction on nanoclay modified asphalt binders, were conducted by me.

Chapter 3 of this work has been published as L. Monteiro, M. Shafiee, L. Hashemian and O. Maadani, "Rheological and Self-Healing Properties of Asphalt Binders Modified using Nanoclay" in the CTAA 66th Annual Conference and Annual General Meeting held virtually. The work was presented on November 16, 2021. Dr. Leila Hashemian and Dr. Mohammed Shafiee were responsible for the conception of the study, while I was responsible for the data collection and draft preparation. All authors were responsible for the data analysis, draft review, and approving the manuscript's final version.

Chapter 4 of this research has been submitted for publication. It is at this moment under review as L. Monteiro, K. Freed, M. Shafiee, O. Maadani and L. Hashemian, "Investigation of Self-healing Properties of Nanoclay Modified Asphalt Binder using Two-Piece Healing Test" in the Canadian Journal of Civil Engineering. The work conception was prepared by Dr. Leila Hashemian and Mohammed Shafiee, while Kalen Freed and I were responsible for material preparation and data collection. I was responsible for the draft preparation. All authors were responsible for the data analysis and approval of the final version of the manuscript.

Chapter 5 of this research has been submitted for publication. It is at this moment under review as L. Monteiro, T.B. Moghaddam, M. Shafiee and L. Hashemian, " Investigation of Laboratory Aging Effects on Nanoclay-Modified Asphalt Binders" in the Construction and Building Materials Journal. The work conception was prepared by Dr. Leila Hashemian and Mohammed Shafiee, while I was responsible for data collection and the first draft. All authors were responsible for the final version of the manuscript.

Chapter 6 is composed of a summary and conclusions of this work.

Acknowledgments

I would like to recognize my supervisor's great work, Dr. Leila Hashemian. She has worked so hard throughout my research, giving me her attention when needed, including weekends, holidays, and past work hours. She acknowledged my needs and provided all the resources I needed to complete my work in a non-stressful manner.

I would also like to recognize my colleagues Farshad Kamran, Amirhossein Ghasemirad, Mohamed Saleh, Taher Baghaee Moghaddam, Thomas Johnson and Kalen Freed for the many hours working together.

Also, I would like to extend my appreciation to my colleagues Farshad Kamran, Amirhossein Ghasemirad, Mohamed Saleh, Manjunath Basavarajappa, Sabrina Rashid, Nusrat Jhora and Muhammad Misbah, who made our work hours enjoyable.

I would like to acknowledge the financial assistance of the National Research Council of Canada. I would also like to thank Mohamed Shafiee for helping me with the work conception and review and being such an accessible person. Also, Omran Maadani, for the great insights on this work.

Finally, I am grateful for my parents, Luis Claudio and Neide Neves and my fiancée Camila Alvarenga, who have always been with me. A special thanks to my friends Cassio and Fernanda Imamura, who have been so supportive towards me, and thanks to my friends Nathalia Couto, Luiz Biagini and Bruna Dutra.

Table of Contents

List of Tables

List of Figures

1 Introduction

Flexible pavement accounts for most of the paved network in Canada. Pavement degrades over time due to environmental impacts and increased traffic load repetitions. This degradation is revealed in several forms: permanent deformation (rutting), fatigue cracking, and low-temperature cracking. These distresses reduce the pavement's durability and lifespan [1]. Considering the impacts of climate change and increasing traffic loads in Canada, flexible pavements are subject to unprecedented deterioration and reduced service life. In this regard, asphalt binder characteristics play an essential role in the overall short-term and long-term performance of asphalt pavement. The asphalt exhibits properties to resist distresses caused by weathering and traffic loads. Improving the asphalt binder material could lead to more resilient pavements, capable of sustaining future increases in environmental and loading impacts.

Asphalt binder is a self-healing material, meaning that it can self-recover its properties after damage [2]. A self-healing material has a mechanism similar to those seen in animals and plants, such as recovering function by a broken bone over a rest period [3]. Healing must have a trigger that can be either extrinsic (with the aid of an external agent) or intrinsic (inherent ability). It was first observed in the 1960s by Bazin and Saunier that asphalt binder has an intrinsic ability to self-recover [4]. The intrinsic healing process has two modes: short-term healing, which is due to wetting (the complete interaction between the surfaces adjacent to the crack), and long-term recovery, which is attributed to the randomization of molecules around damaged surfaces inter-diffusion of molecules [4–6].

Asphalt binder modification is a notable method for more resilient asphalt pavements. Studies on Styrene-Butadiene-Styrene (SBS) modified binders have shown that the inclusion of SBS improves the rutting, low-temperature and healing behaviour of asphalt mixtures [7,8]. Also, Gilsonite-[9,10], Polyethylene- [7,9] and crumb rubber [9,10] exhibited improved rutting and fatigue resistances but degraded the healing behaviour of the asphalt mixtures. Although

SBS-modified binders help improve specific properties, the high construction cost, reduced ageing resistance and storage stability are challenges to overcome [11–13]. Nanotechnology is a relatively new trend in asphalt, and nanoclay-modified binder is a promising solution for improving pavement resistance.

Common clays can be divided into four groups: kaolinite, montmorillonite (MMT), illite, and chlorite [14]. Among these, MMT is the most common, and it is used as a filler in various materials [15]. Clays, it should be noted, are characterized by their layer arrangements, which are made up of tetrahedral and octahedral bond angles [15]. The most notable characteristic of these clays is the Cation Exchange Capacity (CEC), and it is also an essential property in terms of the performance of nanoclays as modifiers [14]. As with most clays, MMT is hydrophilic and has poor asphalt dispersion [14]. Asphalt compatible clays are produced through surface modification of MMT with an organic chemical capable of bonding to the surface of the layers, when dispersed present layered silicates of 1 nm thickness [14].

Nanoclays are cheaper than SBS when surface-modified are compatible with asphalt, and studies have shown traits indicating higher work of cohesion [11] and fatigue life [16]. These characteristics suggest that nanoclay could lead to more durable asphalt pavement.

1.1 Objectives

This research aims to study the rheological (with focus on ageing and fatigue), mechanical, and healing properties of nanoclay modified asphalt binders and mixtures. In this regard, two organo-modified montmorillonites were incorporated into an asphalt binder and investigated for mixture method effectiveness, storage stability, performance grading in high, intermediate, and low temperatures. Also, the healing properties and ageing behaviours of the nanoclay-modified binder were assessed. On a larger scale, asphalt mixtures were also studied; hot-mix asphalts (HMAs) were prepared at their optimum binder contents, then the mixes were subjected to fatigue and healing tests. Investigating asphalt binders and mixtures

provides a more comprehensive understanding of the impact of nanoclay incorporation on the rheological and mechanical properties in the flexible pavements.

1.2 Methodology

A PG 64-28 neat (original) binder was mixed with Cloisite 15 A nanoclay (2% and 4% by weight of the binder) and Cloisite 20 A nanoclay (2% and 4% by weight of the binder) using a high shear mix to produce four nanoclay-modified binders. The dispersion of the nanoclays in the binder was analyzed by employing a scanning electron microscope.

The binders were subject to Superpave performance tests, SARA fraction, Frequency-Sweep test, two-piece healing test, and steady shear flow test.

At the asphalt mixture level, the addition of nanoclay was investigated by using the four-point bending fatigue test for healing, dynamic modulus test, and Marshall flow and stability test.

1.3 Thesis Structure

This paper-based thesis is organized into six (6) chapters:

Chapter 1 - Introduction: This chapter gives a brief background of the scope of work, outlines motives for this research, and highlights the objectives, methodology and thesis structure.

Chapter 2 - Literature Review: The asphalt binder compositions, properties, investigation methods and modifiers are discussed. Also, relevant studies on the asphalt mixture compositions, properties and investigation methods with the focus on the healing properties were provided.

Chapter 3 - Rheological and Self-Healing Properties of Asphalt Binders Modified using Nanoclay: The performance grading of modified asphalt binders were found, then using a two-piece healing test, the self-healing behaviour of nanoclay-modified asphalt binders were determined.

Chapter 4 - Investigation of Self-healing Properties of Nanoclay Modified Asphalt Binder using Two-Piece Healing Test: The complex shear modulus of a healing asphalt is compared with different nanoclay-modified binders with the comparison between instant and over-time healing.

Chapter 5 – Investigation of Laboratory Aging Effects on Nanoclay-Modified Asphalt Binders: The storage stability studied using SARA fractions, and the impact of nanoclay modification is investigated by employing frequency-sweep test and development of master curves.

Chapter 6 – Summary and Conclusions: The impact of using Cloisite 15A nanoclay (2% and 4% by weight of binder) and Cloisite 20A nanoclay (2% and 4% by weight of binder) on asphalt rheology, healing behaviour, and asphalt ageing are summarized.

2 Literature Review

2.1 Asphalt Binder

Asphalt binder or asphalt cement, as known in North America, is also called "Bitumen" in Europe and other parts of the world. In this work, the North American versions is used.

Asphalt binder has many applications, but most commonly, it is used as a construction material for pavements. Pavements are subjected to various loads and conditions, by which their resistance to them are primarily dependent on the quantity and properties of the asphalt binder. Asphalt binders are complex heterogeneous mixtures of hydrocarbons, typically composed of 82%–88% carbon, 8%–11% hydrogen, 0%–6% sulphur, 0%–1.5% oxygen, and 0%–1% nitrogen [1,17]. Asphalt is a viscoelastic material, meaning that depending on the temperature and time combination, it can exhibit a behaviour that is either: viscous, elastic or a combination of both. It can be inferred that the behaviour exhibited by the binder in high temperatures over short periods is equivalent to that seen in low temperatures over long periods. This concept is known as the time-temperature superposition (TTS), commonly used to analyze the behaviour of asphalt over different temperatures, frequencies and conditions [18].

Asphalt is produced from the distillation of crude oil, and it is manufactured to meet grade specifications by refining or blending [19]. The most commonly used asphalt mixture and analysis method in Canada is the Superpave system, which stands for Superior Performing Asphalt Pavements. Superpave includes a performance-based system for specifications of asphalt binders, aggregates, hot mix asphalt and testing [20].

The Superpave performance grade (PG) is a two-number characterization of a binder. The first number indicates the average seven-day maximum design temperature (in °C), while the second number represents the minimum design temperature (in °C) to be experienced by the pavement.

Asphalt conditioning is an essential part of asphalt grading, as it measures the impact of heat, air, oxidation and time on the binder. The Rolling Thin-Film Oven (RTFO) test is a conditioning method through heat and air on a moving film of asphalt, representing an approximation of a binder immediately after constructing a pavement. This short-term ageing is conducted according to AASHTO 240-13. Samples weighing 35 ± 0.5 g of the binder are poured into each bottle before a rest period at room temperature. The ageing procedure takes 85 minutes inside the RTFO oven, with a temperature setting of 163 °C, with the bottles being rotated at a rate of 15 ± 0.2 r/min and 4000 ± 300 mL/min airflow [21]. The RTFO used in this study is shown in Figure 2-1.

Figure 2-1. Rolling Thin-Film Oven

Another critical condition that must be analyzed in asphalt is long-term ageing, for which behaviours such as life cycles and low-temperature cracking resistance are investigated. This over-time ageing is conducted in asphalt binders following AASHTO R 28-12. This procedure is designed to simulate the in-service oxidative ageing during an asphalt pavement's service life. This test is called the pressure ageing vessel (PAV), by which RTFO-aged samples are

conditioned for 20 hours in a pressurized vessel with air 2.10 MPa at 100°C, then vacuum degassed. The samples obtained from this test are further investigated to estimate the properties of asphalt after 5 to 10 years of pavement service [22]. A PAV and vacuum oven used for ageing are shown in Figure 2-2, at parts a and b, respectively.

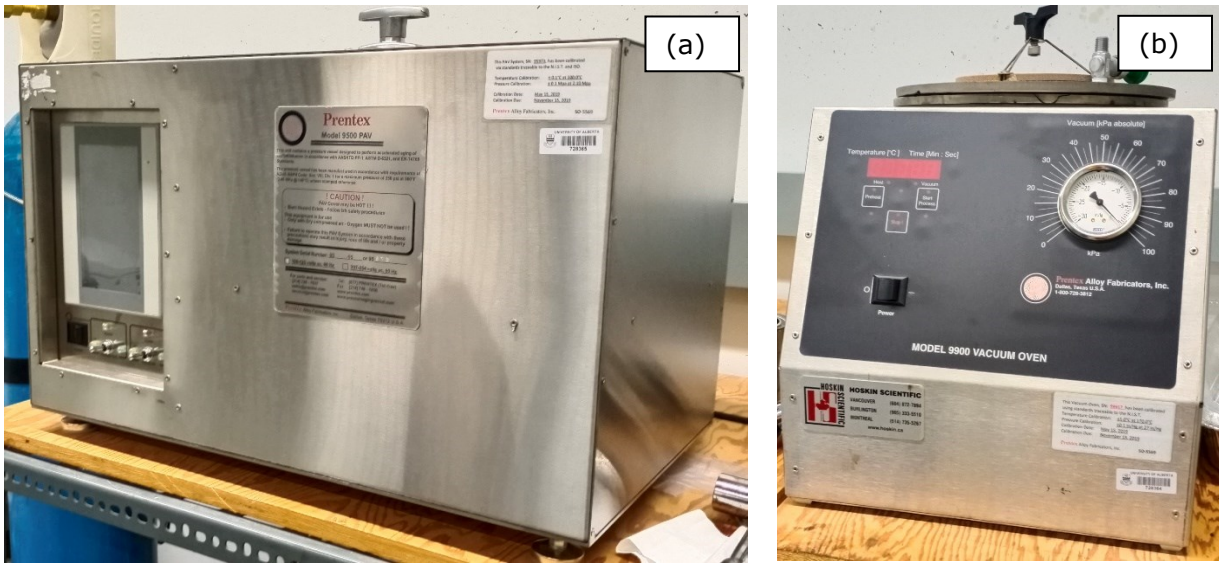

Figure 2-2. (a) Pressure Aging Vessel, (b) Vacuum Oven

The PG-grading of a binder is conducted following steps as listed in AASHTO R 29-15 [23], which indicates the original high-temperature verification for a binder as the first-grade investigation. This test is conducted, following AASHTO T 315-20 [24] on an asphalt sample, using a Dynamic Shear Rheometer (DSR), as seen in Figure 2-3. The complex shear modulus (G*) and phase angle (δ) of the binder are measured starting at 58 °C, then at an increment or reduction of 6 °C test temperature, until the $G^*/\sin(\delta) \leq 1.0$ KPa. The high grade is specified by AASHTO M 320-17 [25] as the highest grade by which the $G^*/\sin(\delta) \geq 1.0$ KPa.

Figure 2-3. Dynamic Shear Rheometer

Following the initial binder grading, the RTFO-aged asphalt is subjected to the same testing procedure according to AASHTO T 315-20 [24], with a difference in the magnitude of G*/sin(δ) changing from 1.0 KPa to 2.2 KPa. The lowest value between the original and RTFO-aged binders is the high-temperature grade.

The PAV-aging of the asphalt binders should be conducted on RTFO-aged binders after the conduction of the high-temperature grading. The high grade determines the temperature at which the binder should be aged, 90 ºC for PG 46-xx and PG 52-xx and 100 ºC for higher grade binders (Binders used in desert climate should be PAV-aged at 110 ºC) [22].

Intermediate temperature behaviour is also analyzed, but the value obtained in testing is not utilized in the grade. The investigation of the intermediate behaviour is conducted on the PAV-aged binders according to AASHTO T 315-20 [24] using a DSR. The temperatures at which the binder should be tested are listed in AASHTO M 320-17 [25], and the failure temperature is when G* x sin(δ) > 5,000 KPa.

The low-temperature grade is found by conducting the bending beam rheometer (BBR) test according to AASHTO T 313-12 [26]. The test is performed on the PAV-aged samples and at a temperature specified by AASHTO M 320-17 [25]. The verifying temperature of the binder should be 10ºC higher than the grade; for example, a PG xx-28 low-temperature is tested at -18 ºC [23]. The criteria for the low grade, as specified by AASHTO M 320-17 [25], is the lowest temperature where the creep stiffness (S) ≤ 300 MPa and the slope value, m, ≥ .300. If S is between 300 MPa and MPa, while the m criteria have been satisfied, it may be possible to comply with the requirements by using a direct tension test on six different samples [23]. Figure 2-4 shows the BBR equipment used at the University of Alberta Pavement laboratories. After conducting the BBR test on two separate specimens, a master curve is constructed according to AASHTO R 49-09 [12]. A low-temperature failure grade is found and, therefore, the PG-grade characterization of the binder.

Figure 2-4. Bending Beam Rheometer

The Superpave method also highlights using a Rotational Viscometer (RV) as the toolset to encounter the desired for and unmodified binder's mixing and compaction temperatures of

hot asphalt mixtures. According to AASHTO T316-20, an RV, such as the one shown in Figure 2-5, is employed to measure the apparent viscosity of the asphalt binder at usage temperatures. Viscosity readings are taken from the device at 1-minute intervals for 3 minutes for each temperature [27]. The results are plotted, and there the viscosities are 0.17 ± 0.02 Pa-s and 0.28 ± 0.03 Pa-s, representing the mixing and compaction temperature ranges, respectively [28].

Figure 2-5. Rotation Viscometer

Studies have shown that the use of an RV is not recommended for mixing and compaction temperatures of modified asphalt binders [29,30]; instead, alternative methods have been recommended by the National Cooperative Highway Research Program (NCHRP)[28]. DSR is the equipment used for both proposed alternatives, which are called: the phase angle and steady shear flow methods [28].

The phase angle method is one way to determine temperatures for proper mixing and aggregate coating. Frequency-sweep tests are conducted through DSR, where both G* and

phase angle data are collected for at least 3 temperatures, one of which is 80ºC. This test consists of three steps for the analysis: a graph of G* and δ over frequency, then creating a master curve at the reference temperature 80ºC, followed by identifying the frequency where the δ crosses 86 º. The mixing temperature is defined by equation (2-1) and the compaction temperature by equation (2-2) [28].

$$Mixing\ Temperature\ (°F) = 325w^{-0.0135} \quad (2\text{-}1)$$

$$Compaction\ Temperature\ (°F) = 300w^{-0.012} \quad (2\text{-}2)$$

The steady shear flow method adopts a range of viscosity to find the mixing and compaction temperatures, such as the one used for Superpave by employing an RV. An unaged binder is subjected to a test flow mode over a range of shear stresses from 0 to 500 Pa at three temperatures (76, 82 and 88ºC). The viscosity results for each temperature at 500 Pa are plotted. The mixing temperature range is where the viscosity is between 0.15 to 0.19 Pa-s, while the compaction temperature range is when viscosity is between 0.32 and 0.38 Pa-s [28].

Performance grading is one perception of identifying a binder that will fulfill the design parameters of the asphalt mixture. Still, it does not fully characterize the behaviour presented by the mixture. Asphalt is a temperature-sensitive viscoelastic material, by which the relation between the mechanical properties, temperature and time of loading is known at the time-temperature superposition principle [31]. The DSR is a tool by which viscoelastic material properties can be obtained. G* is the maximum stress ratio to maximum strain, and it shows the resistance of a material to deformation. Another property used to analyze asphalt binders is the δ, which represents the time lag between the stress and strain of the asphalt during a test condition. It defines the viscous and elastic properties of materials [32]. Employing the DSR under various frequencies and temperatures of asphalt, a master curve can be created using a TTS shift-factor on a reference temperature, and therefore through one curve, convert

the rheological properties of a material at one temperature and loading frequency to the properties at another temperature and loading frequency [31].

2.2 Asphalt Mixture

The Superpave HMA design requires the conformance to properties such as: bulk specific gravity, maximum theoretical specific gravity and volume of air voids. The bulk specific gravity of bituminous mixtures (G_{mb}) is found by following the AASHTO T 166 [33]. The bulk specific gravity test finds the compacted HMA weight under three conditions: dry, saturated surface dry (SSD), and submerged. The maximum theoretical specific gravity (G_{mm}) is found by using loose HMA according to AASHTO T 209-12 [34]. The loose asphalt weight is found under dry and submerged conditions after vacuum sealed. Both the G_{mb} and G_{mm} are used to find the volume of air voids present in the asphalt mixture.

The dynamic modulus test can calculate various properties in asphalt mixtures, including the dynamic modulus. According to AASHTO T378, an universal testing machine (UTM) applies compressive stress to cylindrical asphalt samples under different temperatures and frequencies [35]. Using the same TTSP concept applied in the binders, a master curve can be created at a reference temperature to characterize the mixture under a broader range of temperatures and frequencies, following AASHTO R87 [36]. The dynamic modulus samples are compacted with a Superpave gyratory compactor (SGC) to dimensions of 150 mm diameter by 170 mm height. The SGC samples are subjected to a coring device then to an electrical saw to produce a final specimen with measurements of 100 mm diameter by 150 mm height. Linear variable displacement transducers (LVDTs) are attached to the sample using a fixing modulus jig. The LVDTs are used to measure the midspan vertical deflection of the sample during the dynamic modulus test as seen in Figure 2-6.

Figure 2-6. Dynamic Modulus Sample

Investigating the fatigue life of asphalt mixtures is one method to compare the impact modifiers on improvements on asphalt mixtures. The four-point bending apparatus as seen in Figure 2-7 is used to determine the asphalt beams' fatigue life and failure energy according to AASHTO T 321-17 [37]. Asphalt slabs with 400 mm length, 300 mm width and 65 mm height are compacted. Using an electric saw, each of these slabs is cut into beams with dimensions of 380 mm length, by 50 mm width and 65 mm height. A nut is attached to the center of the beam; then, the beam is tested using the four-point bending apparatus until it reaches fatigue.

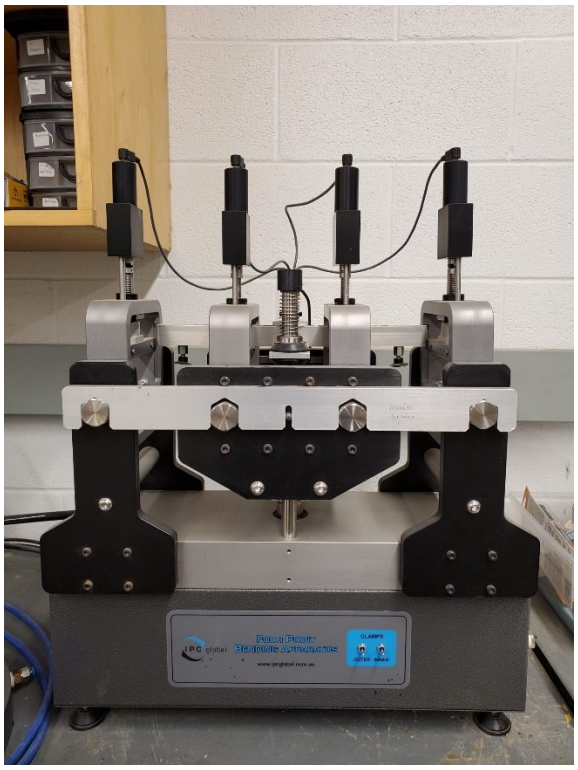

Figure 2-7. Four-Point Bending Apparatus

2.3 Self-healing Materials

Damage is the incurrence of new micro and macro cracks into a material, detrimental to its properties. The damage formation is not problematic if it is accompanied by healing [38].

Healing is a phenomenon that occurs on materials, and during its service life, there is competition on its rate of damage versus its rate of healing [38]. Self-healing materials can repair themselves after the incurrence of cracks, triggered by the damage autonomously or by external factors [39]. These healing materials can be divided into three major categories: i) Capsule based, ii) Vascular and iii) Intrinsic.

Capsule-based self-healing materials comprise capsules that are dispersed on the matrix of the material. The capsules break upon material damage, releasing a healing agent with low viscosity and repairing the nano- and micro- cracks. Because of the nature of the capsules, the material can only heal once [40]. Figure 2-8 demonstrates the process of healing by the use of capsules [41].

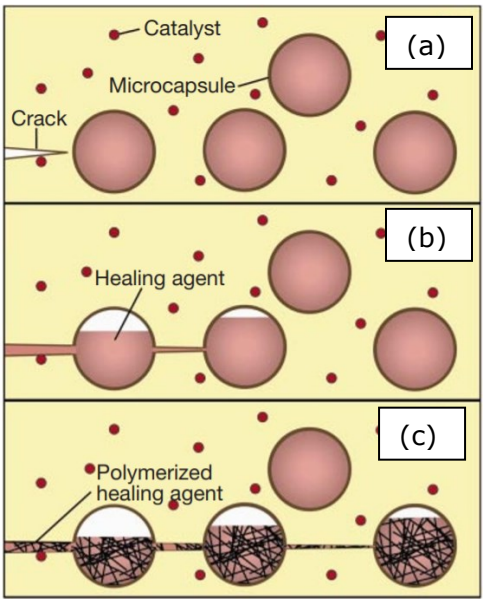

Figure 2-8. Capsule base healing (a) crack formation, (b) release of healing agent, (c) polymerisation and crack closure

Source: White, 2010

Vascular healing materials mimic the repairing behaviour of the human body. It composes the matrix of the material of a network of capillaries filled with a healing agent, which would be released upon damage. Because of the link between capillaries, it is expected from the material to repair itself upon damage several times [42]. Figure 2-9 shows the process followed by the microvascular healing, by which the capillaries rupture and heal the asphalt [43].

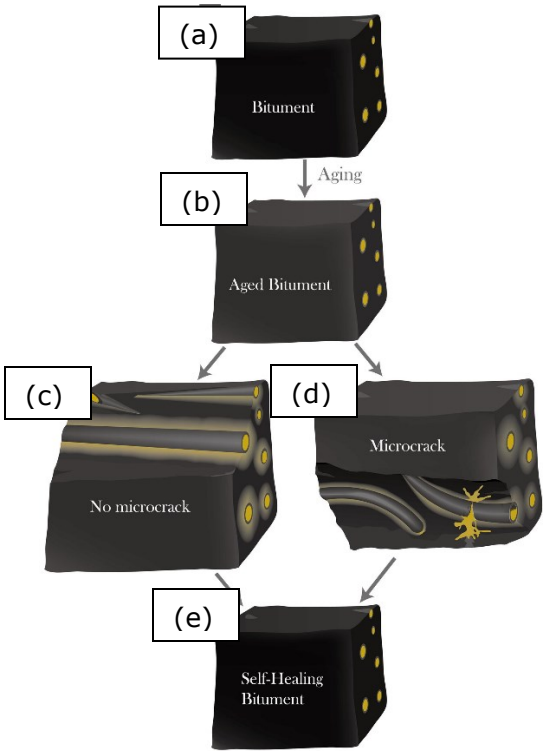

Figure 2-9. Vascular healing: (a) unaged binder, (b) aged binder, (c) binder before cracks, (d) microcrack formation and healing agent released, (e) healed binder

Source: Zhang et al., 2018

Intrinsic self-healing materials can repair themselves by their essence, and the healing phenomenon is followed by the presented order: surface rearrangement, surface approach, wetting, diffusion, and randomization of molecules. The materials' mechanical properties' recovery is seen during the wetting and diffusion stages of healing [44]. Figure 2-10 demonstrates the process an intrinsic healing material follows when micro-cracks appear [45].

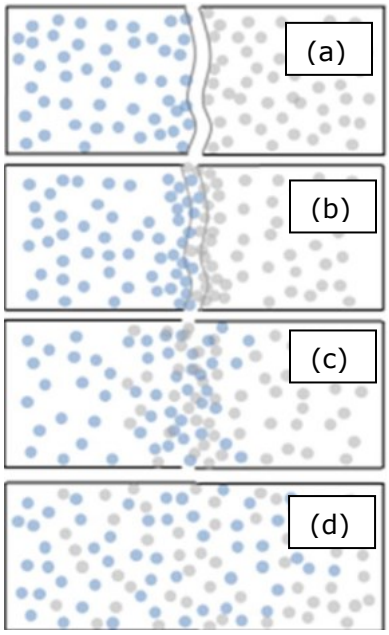

Figure 2-10. Instrinsic healing: (a) surface rearrangement and aproach, (b) wetting, (c) diffusion of molecules, (d) randomization of molecules

Source: Liang et al., 2021

2.4 Self-Healing in Asphalt

Asphalt binder is considered an intrinsic self-healing material, by which the triggering mechanism is its matrix essence [6]. After removing an external load from the asphalt binder, two processes will be followed instantaneously: viscoelastic recovery and healing. The fundamental differences between them are that the viscoelastic recovery is due to the randomization of the molecules with the matrix and triggers independently of the load intensity. At the same time, healing is due to wetting and diffusion of molecules from the nano crack faces, and the phenomenon is triggered when the external load causes damage [46]. Little and Bhasin describe self-healing in asphalt in three stages: complete contact of crack surfaces, interdiffusion of molecules from two cracked surfaces, and the randomization of the molecules within the matrix to rearrange to original material structure [46].

Although the asphalt has an intrinsic behaviour of recovering mechanical properties after damage, several internal and external factors influence that phenomenon. A low softening

point increases the healing behaviour of the asphalt binder, as it is the point where it reaches its full potential [47]. Ageing harms healing by increasing the optimum healing temperature, decreasing the possibility of crack diminishing at asphalt pavement temperatures[47].

Santagata et al. reported that a higher saturate to aromatics ratio (S/Ar) increases the healing ability of asphalt [8]. Sun et al. went further on the study. They concluded that even though a higher S/Ar increases the healing potential, a high aromatic concentration shows high healing potential. The molecule structure has more influence than the molecule content [48].

Bommavaram et al. described that wetting, the rapid gain of strength in healing, is because of the work of cohesion of the asphalt matrix [49]. Most of the cracks on asphalt mixture occur either on the asphalt-aggregate interface or in the asphalt-asphalt interface, related to the adhesion and cohesion forces of the variety respectfully. Surface free energy has a tool to determine the gain of strength and adhesion in the healing process of asphalt mixtures [50].

Studies have shown that introducing rest periods to the asphalt pavement increases the healing phenomenon of the asphalt [51,52].The diffusion period of healing is time-dependent, so as some strength will be regained through wetting, it is expected that the mechanical properties recover because of molecules' interfusion over time [5,53]. At constant temperatures, asphalt binder can repair micro-cracks, by which this phenomenon can fully recover the asphalt mechanical properties if enough heat energy is applied. Low temperatures take higher energy and time to inter-diffuse asphalt molecules, and temperatures that are too high cause permanent deformation to the asphalt mixture; hence there are optimum healing temperatures to recover properties at full potential [54].

Ageing significantly reduces the healing potential of asphalt as it increases its softening point, reducing the flow of the molecules and requiring more energy to repair cracks found in the matrix [55]. It has been studied and confirmed that the damage level matters in healing, with

nano- and micro-cracks being much more inclined to heal fully than meso- and macro-cracks [6,51,56].

Various asphalt modifiers have been investigated for their healing behaviours with improving and worsening effects. Including Styrene-Butadiene-Styrene (SBS) has shown better results of healing when compared with a neat binder. Still, its poor compatibility with asphalt, poor storage performance, low resistance to Ultra Violet (UV) light, and high costs impose obstacles to its implementation on a large scale to improve the self-healing of asphalt [57,58].

2.5 Nanoclays

Clays are naturally occurring layered silicates that can be interlaid in 1:1 or 2:1 structures and broadly subdivided into three major groups: Montmorillonite, Kaolinite/Smectite, and Illite [59]. There are two types of clay layers: tetrahedral and octahedral. While the first is structured with SiO_4 silicon-oxygen tetrahedra, the alumina AlO_6 octahedral layers are either aluminum or magnesium with hydroxyl. Except for the kaolinites, clays are 2:1 structures by which there are two layers of tetrahedral sheets evolving the octahedral sheet [14].

Nanoclays are the nanoparticles of these mineral silicates by which their layers are measured in the nanoscale. Montmorillonite is the most industrially used nanoclay, and its aluminosilicate layers are approximately 1 nm thick [60]. One of the primary sources of Montmorillonite in nature, Bentonite nanoclay, often has in its composition quartz, Illite, carbonites chlorite, and mica [61].

When dispersed in asphalt, Nanoclays can present three types of structures: conventional, intercalated, and exfoliated. In conventional dispersion, the nanoclay particles are scattered throughout the matrix, maintaining their original networks in agglomerates with no intercalation of the asphalt binder between the layered silicates. Intercalated nanoclay dispersion presents a good distribution of the nanoparticles throughout the matrix, maintaining the original silicate structures with polymers penetrating between the silicates. At exfoliated nanoclay-asphalt dispersal, the tetrahedral and octahedral layers of the nanoclay

have been segregated, and there is high intercalation between the silica layers and the binder [15,62].

In nature, clays are mostly hydrophilic silicates, and to get a good dispersion with a polymer such as an asphalt binder, the clay must have its surface polarity modified [63]. These organophilic silicates are produced by ion exchange between the clay and the modifiers. Cloisite® 15A and Cloisite® 20A are respectively quaternary ammonium salt octadecyl ammonium chloride-modified montmorillonites and dimethyl, dehydrogenated tallow, quaternary ammonium-modified montmorillonites produced by Southern Clay Products. Choosing the correct organo-modifier for the nanoclay enhances the dispersion by allowing the polymer matrix to penetrate through the silicate layer by intercalation or exfoliation [63].

Cellulose nanocrystal (CNC) are biologically produced nanofibers with dimensions ranging from 10 to 20 nm and high mechanical properties [64]. CNC is a candidate to be used as a modifier for asphalt binders, but dispersion and impact on performance must be investigated.

One of the challenges of using nanomaterial for asphalt modification is the incorporation. For this study, a high shear mixer was employed to add modified asphalt with nanoclays. Although studies using a mechanical mixer [65], an ultrasonic mixer [66] and a paddle mixer [67] have shown that this equipment can successfully incorporate nanoclays into asphalt, comparison studies have shown the high shear mixer to be a more appropriate method [12,68,69].

The investigation of the nanoclay dispersion in the asphalt matrix can be analyzed quantitatively, chemically, or qualitatively. X-ray diffraction (XRD) is a tool often used by researchers to have a quantitative analysis of the interlayer gallery spacing of the nanoclays after mixing. It is also used to determine the dispersion of the nanoclays in the binder matrix [70]. This analysis is done by testing both the control and the modified binders, by which the outputs are given in the form of graphs. The peaks of each chart are compared, and the difference indicates the agglomeration, intercalation or exfoliation [70].

The Fourier transform infrared (FTIR) instruments have been used to analyze the dispersion of asphalt by chemically analyzing the FTIR absorbance of carbonyl bonds [71]. Increases in FTIR spectra can be attributed to the rise of interlayer spacing of nanoclays [72].

A qualitative analysis by visual investigation of the nanoclay dispersion has been reported by several studies [72–74]. A scanning electron microscope (SEM) is a helpful tool to investigate the level of distribution of nanoclays, correlating with the analysis obtained from both XRD and FTIR [73,74]. Thin samples of asphalt binder are put on a pin mount, which is goat coated and inserted into SEM equipment such as the one shown in Figure 2-11. Then, images are taken from the sample with a scope of up to 60,000 times.

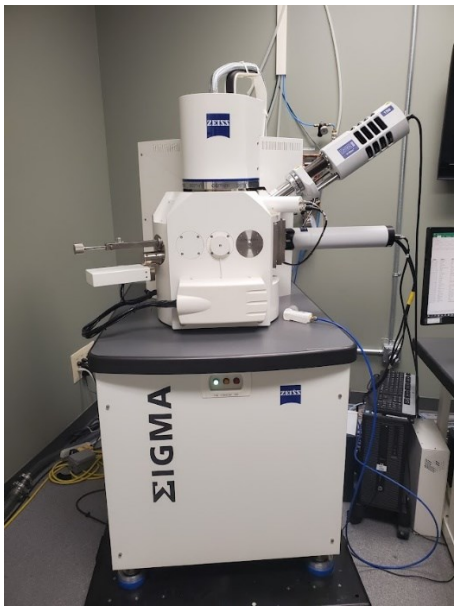

Figure 2-11. Scanning Electron Microscope Equipment

2.6 Asphalt Binder Self-healing test methods

Based on the three steps of the healing process for polymers, Bhasin et al. [5] developed a framework to quantify the intrinsic healing of asphalt binder by steps 2 and 3: interfacial cohesion of the wetted cracked faces and the interdiffusion of the asphalt molecules respectfully. Wool and O'Conner developed the first intrinsic healing function (R_h) for polymers during short-time healing, represented in equation (2-3).

$$R_h(t) = R_0 + Kt^{0.25}x\,\emptyset(t) \quad (2\text{-}3)$$

Where R_0 = initial the instantaneous strength gain due to the second step of the healing process, $Kt^{0.25}x\,\emptyset(t)$ represents the strength gained by the third step, the interdiffusion of the molecules [44]. Using the Avrami equation, Bhasin et al. further developed the equation into equation (2-4).

$$R_h(t) = R_0 + p(1 - e^{-qt^r}) \quad (2\text{-}4)$$

Where q and r = time-independent constants of the healing phenomenon on asphalt, p = healing parameter, t = time (min). The process used to find Rh is called the two-piece healing test (2PH), which analyzes the G* of an asphalt binder specimen of 7 mm during 60 minutes using the DSR, versus the G* of two 3.5 mm samples put in complete contact, simulating a piece of the same thickness, but with cracked surfaces thoroughly wetted [5]. Bhasin et al. noted in their framework that the parameters p, q, and r needed further investigation. Bommavaram and colleagues further developed the equation simplifying the parameter p= 100 – R_0, assuming that hardly will the cracked binder heal its properties to a level higher than before breaking. At the same time, q and r are material properties of the asphalt binder that should be found by a least-squares method. Bommavaram also concluded that R_0 is due to the wetting of the cracked faces, the surface energy, and the cohesion of the molecules [49]. Wang et al. using the same methodology applied in the previous studies, confirmed the relationship between Surface Free Energy and the R_0, showing very similar healing potential [75].

Shen et al. introduced a new method to quantify the healing potential of asphalt binders using the concept of dissipated energy (DE) represented by equation (2-5) and the ratio of dissipated energy change (RDEC) defined by equation (2-6).

$$DE_i = \pi \frac{\sigma^2}{G_i^*} sin\delta_i \quad (2\text{-}5)$$

$$RDEC_n = \frac{(DE_m - DE_n)}{DE_m \, x \, (n - m)} \quad (2\text{-}6)$$

Where DE_i = dissipated energy at cycle i, σ = controlled stress, G_i^* = complex shear modulus, δ_i= phase angle at cycle i, $RDEC_n$ = ratio of dissipated energy at cycle n, DE_m = dissipated energy at cycle m, DE_n = dissipated energy at cycle n, m and n = loading cycles (LC), which m<n. Another coefficient used is the plateau value (PV), representing the RDEC at the cycle in which 50% of the initial showed modulus [76].

Using a dynamic shear Rheometer (DSR), the binder's complex shear modulus (G*), phase angle, stress, and strain are recorded after the introduction of rest periods between intermittent loading sequences. The healing is quantified by the relationship between PV and rest periods (RP), the PV is plotted as the dependent value, while the RP + 1 in seconds is the independent, the slope PV – (RP +1) designates the healing rate, indicating that the higher the PV recovery by seconds of rest time, higher the healing potential [76].

2.7 Asphalt Mixture Self-healing test methods

Shu et al. used a universal testing machine to calculate the healing behaviour of asphalt healing using the three-point bending test (3PB). The healing index evaluated how the asphalt mixtures responded to rest after fractures. The test conducted compared the healing index of both a traditional asphalt mixture and fibre-modified asphalt mixture at various healing temperatures, rest periods, and fracture cycles [77].

Xiang et al. used a variable control method to quantify healing in asphalt mixtures. They were able to find the influence of different healing temperatures, healing times, degrees of damage, and loading strain levels. To evaluate the healing behaviour of the mixes, the four-point bending (4PB) test was followed using AASHTO TP-8 for neat binders and ASTM D7460 for modified binders. Two types of healing index quantify the healing: stiffness healing index, which is the percentage of stiffness recovered by the asphalt mixture after it has healed by the introduction of a determined rest period and fatigue-life healing index, which portion of

loading cycles the healed mixtures can go through before going through fatigue compared to the original undamaged mixture [57]. The method leads to various graphs by which an evaluation can be made about the influence of each factor on the healing behaviour of asphalt mixtures.

To evaluate the effects of ageing on asphalt mixture's self-healing behaviour, Amani et al. used the semi-circular bending test (SCB) at intermediate (25°C) and low (- 20°C) temperatures. The procedure used to quantify healing was similar to the process used in the 4PB test; the healing index for SCB was found by the percentage of energy dissipated to reach fatigue of the asphalt mixtures that was left to heal for 24 hours compared to the necessary power dissipated to get fatigued of a new asphalt mixture. The method compared the healing results at 25°C with the results obtained using the indirect tensile test (IDT), which got similar results [78]. Sakhri et al. used the same procedure to evaluate the self-healing performance of asphalt mixtures containing metal additives [79].

Baaj et al. used a novel method for analyzing healing in asphalt mixtures by using a tension-compression fatigue test in cylindrical samples [80]. Using strain control mode at 10 Hz, a sinusoidal loading is set for a number loading cycles and then a rest period for each sample. The total duration of loading and rest period is 24 hours, that are to be repeated three or four times. The dynamic modulus (E) is measured at the beginning (E_{0i}) and at the end of each loading period (E_{fi}). Each loading period is set to 300,000 cycles, and after the last rest period the sample is loaded until failure. The sample can be tested at various temperatures for the analysis on the impact of temperature on healing. The percentage healed is calculated as $E(_{fi})$-$E(_{0i})/E(_{fi})$ [80].

3 Rheological and Self-Healing Properties of Asphalt Binders Modified using Nanoclay

3.1 Abstract

Increasing traffic loads and climate stressors are key drivers of the deterioration of asphalt concrete pavement. In response to these challenges, asphalt binder modification has gained prominence to improve both the mechanical and the rheological properties of the material. One notable application of asphalt binder modification is the use of nanomaterials, which are capable of altering the asphalt binder at the nanoscale, thereby improving rutting resistance, low-temperature cracking resistance, fatigue resistance, and healing.

In this study, the use of nanoclays for binder modification is investigated in a laboratory setting, focusing on the self-healing behaviour of the binder. The healing potential of nanoclay-modified asphalt is assessed for two different organo-modified montmorillonites at 2 and 4 percent dosages. For this purpose, a two-piece healing test employing a Dynamic Shear Rheometer is used to measure the intrinsic healing behaviour of these binders compared to an unmodified binder. Meanwhile, the effectiveness of the high shear mixing is analyzed using a Scanning Electron Microscope.

It is observed that the complex shear modulus is recovered sooner after cracking when nanoclay is added to the mixture. Overall, this research yields promising results regarding the use of organo-modified montmorillonites as a nano-modifier to reduce asphalt deterioration.

3.2 Introduction

Damage in asphalt pavement typically entails the incurrence of new micro and/or macro cracks in the material that are detrimental to its performance. However, this damage is not irreversible if it is accompanied by healing. In fact, self-healing during the material's service life can slow the rate of overall damage [38]. Healing refers to the intrinsic ability of asphalt to repair itself; recovering its mechanical properties after micro-cracking. The asphalt binder is responsible for the mixture's recovery of properties after cracking, so it can be expected

that improving the healing behaviour of the asphalt binder itself will also improve the healing behaviour of the overall mixture. Although this phenomenon was discovered in the 1960s, the underlying factors are still not well known. What is known is that temperature, aging, and cohesion properties have a strong influence on this phenomenon. Moreover, it is well-established that self-healing in asphalt binder occurs in three stages: wetting (full contact of crack surfaces), interdiffusion of molecules from two cracked surfaces, and the randomization of the molecules within the matrix as they attempt to rearrange into the original material structure [46]. It has also been demonstrated that self-healing is largely governed by the extent of the damage, with nano- and micro-cracks being much more inclined to fully heal than meso- and macro-cracks [6,51,56].

Various asphalt modifiers have been investigated for their role in inducing healing capacity. For example, previous studies have shown that Styrene-Butadiene-Styrene (SBS) can increase healing properties when compared with a neat binder. Nevertheless, other factors, such as its poor compatibility with asphalt, poor storage performance, low resistance to Ultraviolet (UV) light and high cost, hinder its implementation on a large scale in practice [57,58].

Clays, as an alternative modifier, are naturally occurring layered silicates that can be interlaid in 1:1 or 2:1 structures. In terms of mineral composition, clay is broadly subdivided into three major groups: 1) Montmorillonite, 2) Kaolinite/Smectite, and 3) Illite [59]. Nanoclays are defined as silicate minerals whose layers are measurable at the nanoscale. Montmorillonite is the most widely-used nanoclay, with approximately 1-nm-thick aluminosilicate layers [60]. In their natural state, clays are hydrophilic silicates, and, in order to obtain a good dispersion with a hydrophobic asphalt binder, their surface polarities must be modified [63]. In this regard, choosing the correct organo-modifier for the nanoclay enhances the dispersion by allowing the matrix to penetrate through the silicate layer via intercalation or exfoliation [63].

Nanoclays and their application to asphalt pavement have been widely studied, and they have been shown to improve asphalt's resistance to rutting. Organophilic nanoclay-modified binders are storage-stable and highly compatible with asphalt binder [69,81]. A study has shown that nano-modification is 22 to 33 percent lower in cost than polymer modification [11]. A study by Qiu et al., meanwhile, demonstrated that, when microcracks develop, nanoparticles tend to move to the tip of the crack, driven by the high surface energy, thereby arresting the crack propagation [82]. Elsewhere, it has been shown that nanoclays can improve the resistance of Hot Mix Asphalt (HMA) against stripping and fatigue [83]. Cloisite 15A-modified asphalt, for instance, has been shown to exhibit a higher work of cohesion than non-modified asphalt mixtures [84]. As these studies demonstrate, nanoclay-modified asphalt binders show great potential to improve the capacity for self-healing and to extend the service life of asphalt pavement. Reinforcing this idea, Ezzat et al. found that the addition of 3 percent nanosilica improves the self healing behaviour of asphalt [65]. Hossain et al. found that the addition of nanoclays to asphalt binder increases the work of cohesion of the binder, which is a good indicator of healing potential [11]. Tabatabaee and Shafiee, finally, found that, with the introduction of rest periods, organoclay-modified asphalt mixes heal more effectively, and have higher fatigue resistance than non-modified asphalts [85]. Nanoclay-modified binders have not been tested with a well-developed healing test.

Self-healing is a phenomenon defined by the recovery of the asphalt binders' properties, and therefore it can be assessed in various ways. Traditionally, there are two main categories of mechanical healing tests: fatigue-related healing tests, in which the specimen is subjected to intermittent load repetitions followed by rest periods, and fracture-related healing tests, in which healing periods are introduced between two fracture tests [6].

To assess self-healing performance in relation to the binder's properties, Bhasin et al. developed an intrinsic test method called the Two-Piece Healing (TPH) test [5]. In this test, a Dynamic Shear Rheometer (DSR) with a spindle and a base plate of 25-mm diameter are

used to obtain the healing function of the binders tested. TPH mimics the healing behaviour of a binder that is fully cracked and separated. As part of their study, an intrinsic healing function $R_h(t)$, expressed in equation (3-1), was developed by modifying Avrami's equation for describing chemical reaction rates. The analysis is divided into two phases: instantaneous healing due to wetting and interfacial cohesion, represented by the constant R_0, and healing over time due to interfusion and randomization of molecules, represented by $p(1 - e^{-qt^r})$ [5].

$$R_h(t) = R_0 + p(1 - e^{-qt^r}) \quad (3\text{-}1)$$

Subsequent developments led to an improved TPH test framework that provides more specifications for obtaining parameters, p, q, and r, and defining instantaneous healing [49]. Three molds are made, with two featuring cavities 18 mm in diameter and 3.5 mm in height and the third featuring a cavity 18 mm in diameter and 7 mm in height. The asphalt binder was heated and distributed into the molds, then left to rest for 30 minutes. The DSR plate was conditioned to the desired temperature for testing, while the two binders in the smaller molds were attached to the base plate and to the surface of spindle, respectively. The gap between the base plate and the spindle was reduced from 60 to 5 mm, and the apparatus was set up in such a manner as to measure the Complex Shear Modulus (G*) of the binders with minimal interference to the healing process. The test parameters were configured in such a way as to have close to zero normal force application, 0.001 percent strain level, and oscillation of 10 rad/s. The properties were measured specific intervals throughout the course of the 1-hr testing period. After cleaning the device, the binder in the larger mold was attached to the base plate, and the gap was reduced 60 to 5 mm. The control test was run with the identical DSR parameters to mimic the same process with a binder that had not been subjected to cracking. The values were measured at the same intervals during the 1-hr test. A healing percentage (H%) was calculated as defined by Equation (3-2). Due to sample loading and closure of the gap, reading at 1 minute, is considered to be initial testing reading.

$$H\%(t) = \frac{G^*two-piece}{G^*one-piece} \text{x} 100 \quad (3\text{-}2)$$

Where the intrinsic healing constant (R_0) is represented by healing percentage (t=1).

Full recovery of the properties is expected at infinite time, so parameter, p, which is representative of healing over time, can be defined as $100 - R_0$. The constants, q and r, are the asphalt's intrinsic healing properties for inter-diffusion of molecules.

3.3 Objectives and Scope

The objective of the research presented in this paper was to investigate the rheological and self-healing properties of organophilic nanoclay-modified binder. To this end, a High Shear Mixer with hot plate was used to incorporate Cloisite-15A and Cloisite 20A into asphalt. Samples of the nanoclay-modified binders were taken and magnified using a Scanning Electron Microscope (SEM) to ensure proper dispersion of the nanomaterial in the matrix.

To determine the performance grading of the asphalt binders, unaged and Rolling-Thin-Film-Oven (RTFO)-aged samples were tested in the DSR for rutting and fatigue analysis, while Pressure Aging Vessel (PAV) samples were analyzed in a Bending Beam Rheometer (BBR) for low-temperature cracking analysis. Finally, a TPH test was applied to analyze self-healing behaviour; this was carried out by observing unaged binders in the DSR.

3.4 Materials

3.4.1 Binder

The neat binder was a PG 64-28 (supplied by Husky Energy), which is suitable for use in situations where the highest seven-day pavement temperature is no higher than 64°C and the lowest pavement temperature is no lower −28°C. A summary of its properties is provided in Table 3-1.

Table 3-1. Neat Binder Physical and Chemical Properties

Component	Description
Sample Date	July, 2019
Penetration Grade	120/150
Physical state	Liquid
Melting Point / Freezing	> 31°C
Boiling Range	> 228°C (1 atm)
Flash Point	> 243°C (COC)
Density	> 1 kg/L at 15°C
Relative Density	1.020 – 1.040 (Water = 1) at 15°C (1 atm)

3.4.2 Cloisite-15 A Nanoclay

In this study, two types of organophilic phyllosilicate were selected for use in binder modification. The first modifier was Cloisite-15A nanoclay, which is a quaternary ammonium salt-modified natural montmorillonite. This nanomaterial is a rheology additive and, due to its modified nature, is insoluble in water. This Organo-Modified Montmorillonite (OMMT) has an off-white, powdery appearance with a specific gravity of 1.66 g/cc. It has an X-Ray Diffraction d-spacing of 31.5 Å, and is thus considered a nanomaterial. The organic modifier for this Montmorillonite is dimethyl, dihydrogenated tallow, quaternary ammonium with a Cation Exchange Capacity (CEC) of 125 meq/100 g of clay.

3.4.3 Cloisite-20 A Nanoclay

The second nanomaterial chosen for modification was Cloisite-20A nanoclay, also a quaternary ammonium salt-modified natural montmorillonite polymer additive. However, the concentration of the organic modifier dimethyl, dihydrogenated tallow, quaternary ammonium is lower in Cloisite-20A nanoclay, with a CEC value of 95 meq/100 g of clay. Cloisite-20A is an off-white powder intended for use as a polymer additive. The X-Ray diffraction d-spacing of the material is 31.5 Å, with a specific gravity of 1.77 g/cc and a moisture content below 2 percent.

3.5 Preparation of the Nano-modified Binders

The nano-modified binders were prepared using a high shear mixer with a hot plate. Samples with 400 g of PG 64-28 binder were poured into aluminum cans, then placed in a pre-heated oven at 140°C for 30 minutes. The Cloisite-15 A and Cloisite-20 A were separated into bins in batches of 8 g for the 2 percent modifier concentration and 16 g for the 4 percent modifier concentration. A thermometer was inserted into the binder and the can placed on the hot plate, which was adjusted as needed to maintain a binder temperature of 130 ± 2°C. The nanomaterial chosen was then poured into the can and manually mixed for one minute to completely combine it with the binder. The high shear mixer was set to 2,000 rotations per minute for a period of 2 hr and periodically checked for constant temperature. The asphalt binder was mixed in two different concentrations (2 and 4 percent).

3.6 Laboratory Experiments

3.6.1 Scanning Electron Microscope

Improvement of an asphalt binder's properties as a result of modification can only be achieved if the modifier is well dispersed in the matrix. In consideration of this, modified binder samples were subjected to a qualitative evaluation of the dispersion using a Zeiss Sigma Field Emission Scanning Electron Microscope (FESEM). Thin layers of asphalt binder were spread on the surface of the pin mounts with a razor and then sputter-coated with gold using Denton Vacuum gold coating equipment. The samples were then magnified using an FESEM to a magnification scale ranging from 500× to 10,000× to analyze the dispersion of nanoclays.

3.6.2 Dynamic Shear Rheometer – High Temperature Performance Grading

A Smartpave 102 DSR from Antoon Paar was used to investigate the high-performance grading of the nanoclay-modified binders. A spindle with 25-mm diameter was used to complete the tests, as well as silicon molds with cylindrical dimensions of 18-mm diameter and 1-mm thickness. The first set of tests was conducted on unaged binders, which were prepared in accordance with AASHTO T315 to obtain the temperature at which the Complex

Shear Modulus (G*) divided by the sine of the phase shift angle (δ) is greater than 1 kPa at a frequency of 10 rad/s and 12 percent strain. The second set of tests were conducted on RTFO-aged binders in accordance with AASHTO T240 in order to simulate the short-term aging occurring during production and paving. The RTFO-aged specimens were tested in order to obtain the temperature at which G*/sin(δ) greater than or equal to 2.2 kPa at a frequency of 10 rad/s and a 10 percent strain.

3.6.3 Bending Beam Rheometer – Low-Temperature Performance Grading

A Cannon Thermoelectric BBR was used to analyze the low-temperature performance grading of the modified binders in accordance with AASHTO T 313. The RTFO-aged binders were PAV-aged in accordance with AASHTO R 28 in order to simulate 7 to 10 years of service. Asphalt beams were prepared, and their creep stiffness and m-value were measured in order to ascertain the failure temperatures.

3.6.4 Dynamic Shear Rheometer – Two-Piece Healing Test

To investigate self-healing in asphalt binders, a two-piece healing test using an Antoon Paar Smartpave 102 DSR was carried out. This test was conducted in accordance with the framework developed by Bhasin et al. and Bommavaram et al. [5,49] as described above. The test was divided into two steps: a one-piece procedure to obtain the G* of a binder under normal circumstances, and a two-piece procedure to simulate the behaviour of a binder's recovery properties after cracking.

3.6.4.1 One-Piece Procedure

The first procedure was to test a one-piece specimen. An unaged asphalt binder was heated in an oven at 130°C for 30 minutes and poured into a mold with a cylinder cavity of 18-mm diameter and 7.0-mm thickness. The DSR was conditioned to 25°C, while the test parameter was set to a frequency of 10 rad/s and a constant strain amplitude of 0.001 percent in order to minimize interference with the healing process. The specimen also underwent a 30-minute rest period before being attached to the top part of the spindle. The apparatus was then

configured to reduce the gap between the spindle and the bottom plate to 5.0 mm. The complex shear modulus was measured at minutes: 1, 3, 5, 7, 10, 15, 20, 27, 37, 47 and 57. This procedure was repeated six times to ensure repeatability.

3.6.4.2 Two-Piece Procedure

While the one-piece procedure simulates the normal behaviour of an asphalt binder, the two-piece procedure simulates the recovery of G* after full fracture of the binder. For this procedure, unaged binder was heated in an oven at 130°C for 30 minutes, then poured into two molds each with cylinder cavities of 18-mm diameter and 3.5-mm thickness. The DSR configurations used were the same as for the one-piece procedure, with the base plate conditioned at 25°C, but one specimen was attached to the top spindle while the other specimen was attached to the bottom plate. Once again, the procedure was repeated six times to ensure repeatability.

The results obtained from both the one-piece and two-piece procedures were inputted to equation (3-1) in order to obtain R_0 and, consequently, p. The parameters, q and r, meanwhile, were estimated through a process of minimum squared error with the aid of Microsoft Excel's mathematical solver tool.

3.7 Results and Discussion

3.7.1 Dispersion

The analysis of the nanoclays' dispersion in the asphalt binder was conducted for the higher concentration level of each modifier (4 percent). The SEM images show the binder specimens in magnifications ranging from 500× to 20,000×. Figure 3-1(a) shows the asphalt binder with 4 percent Cloisite-15 A, where the absence of agglomerations in the image is indicative of a prominently intercalated and exfoliated matrix and, thus, a successful dispersion. The asphalt binder with 4 percent Cloisite-20 A, shown in Figure 3-1 (b), exhibited a few agglomerations but good dispersion overall.

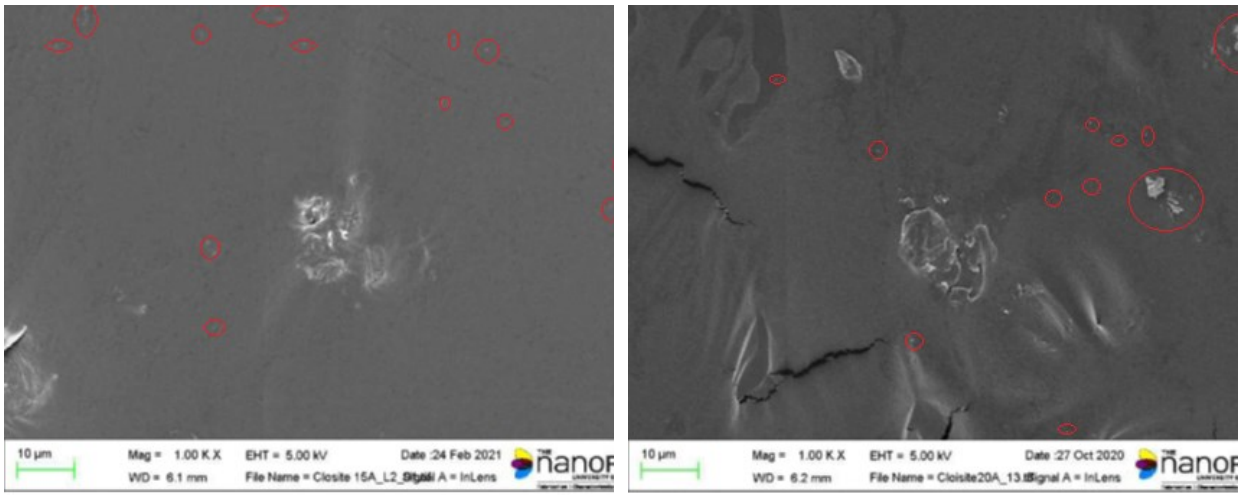

(a) 4% Cloisite-15 A **(b) 4% Cloisite-20 A**

Figure 3-1. Scanning Electron Microscope (SEM) Images of Nanoclay-modified Binders

3.7.2 Performance Grading

3.7.2.1 High-Temperature Performance Grading

The results obtained from the DSR High PG grading are summarized in Table 3-2. High-Temperature Binder Performance Grading (PG). The addition of 2 and 4 percent nanoclay to the binder corresponded with an increase in high-temperature rutting performance for both modifiers. The increase in performance was proportional to the amount of nanoclay added; for 2 percent Cloisite-15 A and 2 percent Cloisite-20 A, increases of 2.4 and 2.8°C, respectively, were observed while no grade increases were observed. Both nanoclays showed performance increases of 5.8°C with the addition of nanoclay at 4 percent concentration, corresponding to an increase in high PG from 64 to 70 for both modifiers.

Table 3-2. High-Temperature Binder Performance Grading (PG)

No.	Asphalt Binder	True High PG (unaged)	True High PG (RTFO-aged binder)	Critical High PG	Difference in Performance	Standard High PG
1	Neat PG 64-28	64.2	65.3	64.2	-	64.0
2	PG 64-28 + 2% Cloisite-15 A	66.6	67.3	66.6	2.4	64.0
3	PG 64-28 + 4% Cloisite-15 A	70.6	70.0	70.0	5.8	70.0
4	PG 64-28 + 2% Cloisite-20 A	67.9	67.0	67.0	2.8	64.0
5	PG 64-28 + 4% Cloisite-20 A	70.0	70.2	70.0	5.8	70.0

3.7.2.2 Low-Temperature Performance Grading

Table 3-3 summarizes the low-performance grading results for the modified and neat binders. The test results show that there were no significant impacts on low-temperature performance as a result of nanoclay modification.

Table 3-3. Low-Temperature Binder Performance Grading (PG)

No.	Asphalt Binder	True Low Temperature (°C) @ 300 MPa	True Low Temperature (°C) @ m_value of .300	Delta critical Temp (°C)	Low Temperature PG	Difference in Performance
1	PG 64-28	−20.6	−22.0	1.4	−30.6	-
2	PG 64-28 + 2% Cloisite-15 A	−20.6	−22.9	2.3	−30.6	-
3	PG 64-28 + 4% Cloisite-15 A	−20.6	−22.8	2.2	−30.6	-
4	PG 64-28 + 2% Cloisite-20 A	−20.3	−22.6	2.3	−30.3	0.3
5	PG 64-28 + 4% Cloisite-20 A	−19.8	−21.7	1.9	−29.8	0.8

3.7.3 Binder Healing Results

The complex shear modulus results for the one-piece and two-piece samples are shown in Table 3 4 and Table 3 5, respectively. These results were used to calculate the H%(t) in accordance with equation (3 2), and this, in turn, was used to calculate the intrinsic function. These results confirm the effect of modified binders in increasing high PG. Moreover, it was

observed that the complex shear modulus increases over time in the case of the two-piece procedure.

Table 3-4. One-Piece Complex Shear Modulus (G*)

Time (minutes)	Neat binder G*(Pa)	2% Cloisite-15 A G*(Pa)	4% Cloisite-15 A G*(Pa)	2% Cloisite-20 A G*(Pa)	4% Cloisite-20 A G*(Pa)
1	8.86E+04	8.89E+04	1.09E+05	1.08E+05	1.63E+05
3	8.31E+04	9.18E+04	1.23E+05	1.22E+05	1.74E+05
5	8.82E+04	1.03E+05	1.28E+05	1.26E+05	1.84E+05
7	9.46E+04	1.11E+05	1.36E+05	1.31E+05	1.60E+05
10	9.79E+04	1.11E+05	1.45E+05	1.30E+05	1.64E+05
15	1.08E+05	1.26E+05	1.53E+05	1.45E+05	1.69E+05
20	1.10E+05	1.33E+05	1.54E+05	1.46E+05	1.64E+05
27	1.11E+05	1.45E+05	1.67E+05	1.45E+05	1.62E+05
37	1.14E+05	1.39E+05	1.65E+05	1.49E+05	1.67E+05
47	1.17E+05	1.36E+05	1.72E+05	1.55E+05	1.84E+05
57	1.14E+05	1.39E+05	1.68E+05	1.54E+05	1.75E+05

Table 3-5. Two-Piece Complex Shear Modulus (G*)

Time (minutes)	Neat binder G*(Pa)	2% Cloisite-15 A G*(Pa)	4% Cloisite-15 A G*(Pa)	2% Cloisite-20 A G*(Pa)	4% Cloisite-20 A G*(Pa)
1	5.77E+04	6.50E+04	9.75E+04	8.44E+04	1.40E+05
3	5.71E+04	7.65E+04	1.06E+05	9.55E+04	1.51E+05
5	5.98E+04	8.01E+04	1.14E+05	1.06E+05	1.63E+05
7	6.25E+04	8.70E+04	1.27E+05	1.14E+05	1.46E+05
10	7.57E+04	9.39E+04	1.29E+05	1.24E+05	1.48E+05
15	7.60E+04	1.06E+05	1.43E+05	1.21E+05	1.53E+05
20	7.91E+04	1.09E+05	1.49E+05	1.23E+05	1.53E+05
27	7.92E+04	1.27E+05	1.53E+05	1.32E+05	1.49E+05
37	8.43E+04	1.16E+05	1.58E+05	1.30E+05	1.58E+05
47	9.09E+04	1.17E+05	1.58E+05	1.25E+05	1.63E+05
57	9.49E+04	1.23E+05	1.62E+05	1.32E+05	1.65E+05

The parameters obtained for the intrinsic healing functions of each binder, shown in Table 3-6, are used to estimate the Intrinsic Healing Percentage (R_h) at any given time. The results show that the nano-modified binders all greatly improved in instantaneous healing properties relative to the neat binder. The 4 percent Cloisite-15 A and 4 percent Cloisite-20 A, showed the most significant change in instantaneous healing, increasing from 65 percent in the neat binder to 90 and 86 percent, respectively.

Table 3-6. Intrinsic Healing Function Parameters

Parameter	Neat Binder	2% Cloisite-15 A	4% Cloisite-15 A	2% Cloisite-20 A	4% Cloisite-20 A
R_0	0.651	0.732	0.897	0.780	0.860
p	0.349	0.268	0.103	0.220	0.140
q	0.033	0.211	0.032	0.317	0.146
r	0.690	0.307	0.815	0.110	0.404

The intrinsic functions are plotted in Figure 3-2, where a significant difference in healing potential can be observed between the neat binder and the nanoclay-modified binder. The 2 percent Cloisite-15 A and 2 percent Cloisite-20 A samples exhibited very similar trends in this regard. Similarly, the 4 percent Cloisite-15 A-modified binders and 4 percent Cloisite-20-modified binders had nearly identical performance.

The overall healing percentages after a 56-minute rest period following a theoretical crack are presented in Figure 3-3.

As can be seen, the addition of Cloisite-15 A resulted in improvements in the self-healing property of the PG 64-28 binder over time, with the higher concentrations corresponding to better results. The 4 percent Cloisite-15 A-modified asphalt nearly fully recovered its properties before cracking at 96 percent healed, compared to 87 percent for the 2 percent Cloisite-15 A and 65 percent for the neat binder. The Cloisite-20 A also exhibited high values of recovery—93 and 87 percent for the 4 and 2 percent concentrations, respectively.

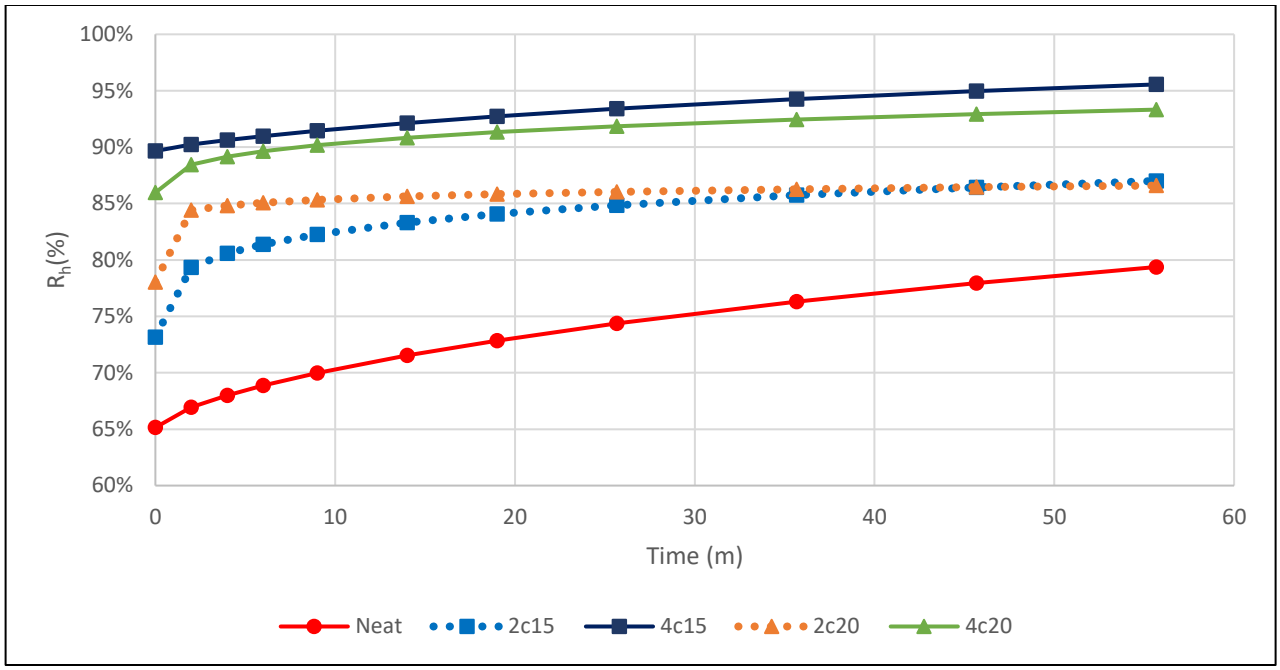

Figure 3-2. Intrinsic Healing Percentage (Rh) of Nanoclay-modified Binders

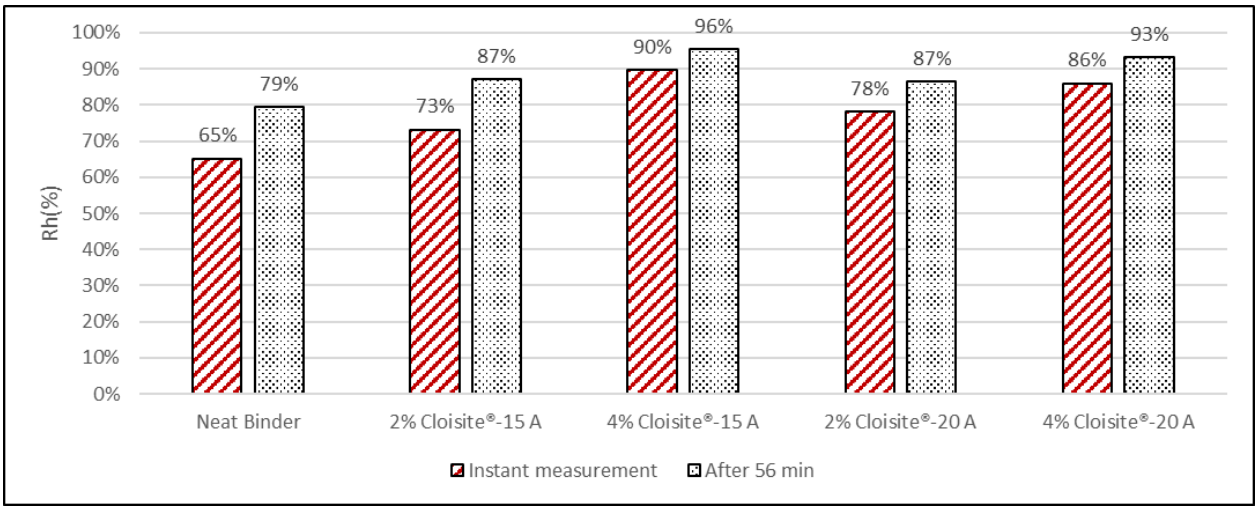

Figure 3-3. Comparison between Instantaneous Healing Percentage (Rh) and Healing over Time

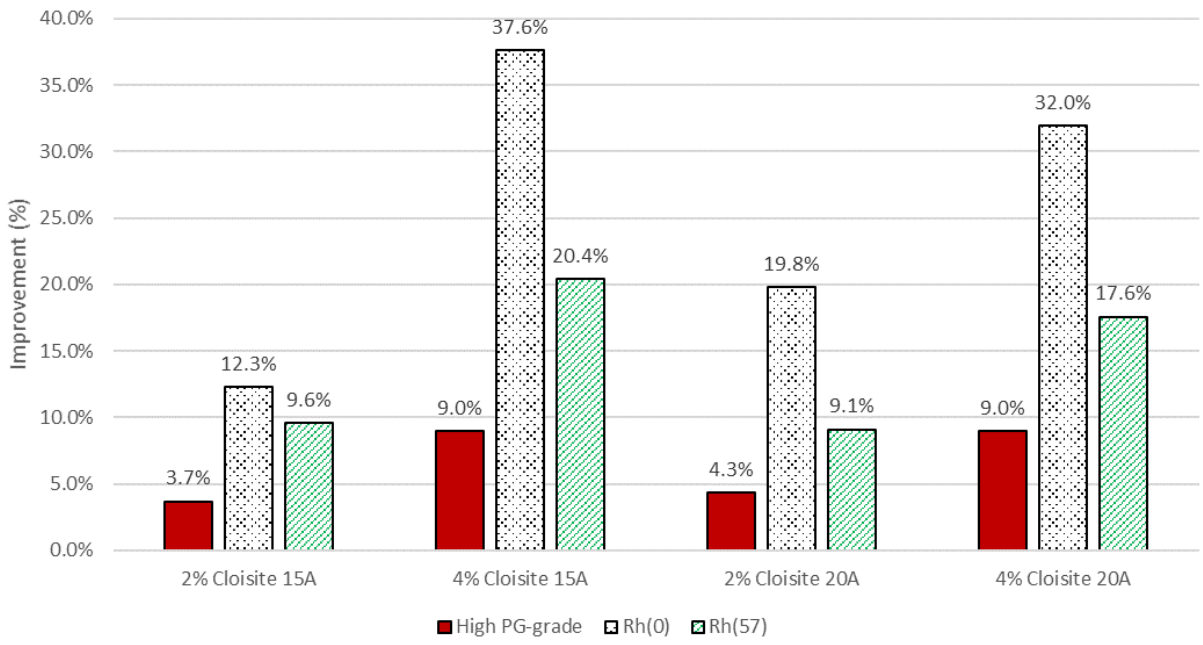

Figure 3-4. Improvements in Nanoclay-modified Binders

The improvements observed in high temperature PG, instantaneous healing, and healing over time of nanoclay-modified asphalt are summarized in Figure 3-4.

The bar chart shows with magnitude the significant improvement in instantaneous healing exhibited by both 4 percent Cloisite-15 A and 4 percent Cloisite-20 A at 37.6 and 32.0 percent, respectively. The chart also shows the significant increase in performance-grading at 9 percent for both nanoclays at 4 percent concentration. It is also worth noting that the modified binders with 4 percent nanoclay exhibited approximately two times the improvement compared to the asphalts with 2 percent concentration of Cloisite-15 A or Cloisite-20 A.

3.8 Conclusions

The objective of this study was to investigate the rheological and self-healing properties of nanoclay-modified binders. To achieve this goal, High Shear Mixing, SEM imaging, DSR high performance grading on unaged binders, DSR High performance grading on RTFO-aged binders, BBR low performance grading on PAV aged binders, and a DSR two-piece healing test were performed.

The findings and conclusions of this work include:

- The SEM showed that the method used in this study for mixing surface-modified montmorillonites provides good dispersion of the material in the matrix.
- The DSR results for high-temperature PG showed that the addition of Cloisite-15 A or Cloisite-20 A increases the high-temperature rutting performance of the asphalt binder proportional to the amount of nanoclay added, with the 4 percent concentrations corresponding to a 5.8°C increase and the 2 percent concentrations corresponding to increases of 2.4 and 2.8°C for the Cloisite-15 A or Cloisite-20 A, respectively.
- The BBR provided values of low-temperature PG, indicating that the addition of nanoclays does not affect the low-temperature cracking performance.
- OMMT improved the intrinsic instantaneous healing of PG 64-28 binders from 12.3 to 19.8 percent at 2 percent concentration and 32 to 37.6 percent at 4 percent concentration.
- Nanoclays improved the intrinsic healing of the binder over time, with the 4 percent Cloisite-15 A-modified binder and 4 percent Cloisite-20 A-modified binder exhibiting recovery levels of 96 and 93 percent, respectively, compared to 79 percent in the case of the neat asphalt binder.
- The Cloisite-15 A and Cloisite-20 A showed promising results in terms of dispersion, high performance grading, low performance grading, and healing.
- Nanoclay modification has great potential to improve the performance of asphalt mixtures, including increases in both the high PG-grade and self-healing of the binder component.

4 Investigation of Self-healing Properties of Nanoclay Modified Asphalt Binder using Two-Piece Healing Test

4.1 Abstract

Asphalt's self-healing properties demonstrate the capability to partially or even fully restore the damage caused by external loads, which could be improved using innovative modifying materials. In this study, the impact of nanoclays on asphalt performance grading, complex shear modulus, and self-healing properties are investigated on a laboratory scale. The intrinsic healing phenomenon of the analyzed binders is measured using a two-piece healing test. Prepared by high shear mixing, the modified binders containing different dosages of two types of organo-modified montmorillonites were evaluated in this paper. In addition to the Superpave performance grading, the dispersion method's effectiveness was analyzed using a Scanning Electron Microscope. This study indicates that nanoclays improve the high-temperature performance grade of the binder while they do not hinder the low-temperature performance. Finally, nanomodified binders showed higher shear strength and improved self-healing properties compared to unmodified binders.

4.2 Introduction

Over 90% of paved roads in the United States and Canada are constructed using asphalt concrete [86,87]. Climate change and the ever-increasing axle loads are detrimental to these asphalt pavements and exacerbate different types of failures such as cracking, ravelling and ageing. It is well-known that self-healing in asphalt is a property that features recovering from damage. Hence it has a significant impact on the overall fatigue resistance of the asphalt pavement [3].

By definition, self-healing indicates a material's capability to partially or fully repair itself after damage during its service life [6]. The recovery of mechanical properties such as strength and stiffness highlights a material's self-healing ability [82]. Previous studies have shown that some asphalt microcracks formed in wintertime can be partially recovered during summer

[82]. In this way, some of the initial strength and stiffness are recovered depending on the asphalt binder's healing rate, which can be broadly subdivided into intrinsic and extrinsic. Extrinsic factors include temperature, degree of damage, compressive stress, ageing, and rest periods [6,88]. On the other hand, chemical composition, viscosity, surface free energy (SFE), and modifiers are among the intrinsic factors of the binder [46,50,82]. The overall healing of asphalt is governed by the binder's properties, SFE, and the geometry of the cracks [89].

One of the common methods for improving the self-healing properties of asphalt is the use of additives [10,54]. Some modifiers can improve the self-healing ability of asphalt by increasing surface free energy and rate of intermolecular reactions and mitigating extrinsic factors such as ageing and damage [11,75,90,91]. The critical factors for a self-healing modifier are asphalt compatibility, high-temperature stability, survivability against the mixing and construction conditions, and capability for continuous or multi-time healing [6].

Given that there are various types of asphalt modifiers, including but not limited to polymers, fibres, chemical agents, and resins, not all can perform great in terms of self-healing. For example, styrene-butadiene-styrene (SBS) may stand out for enhancing the strength and elasticity of asphalt [91], but dramatically increase the binder's overall cost [68]. Over the last decades, nanotechnology has become a growing field in asphalt science. Notably, several researchers tested Montmorillonites (MMT), Bentonites, and Kaolinite for binder modification, and they obtained promising improvements on the rheological properties of asphalt [60,92–94].

In general, clays are broadly subdivided into three major groups, including MMT (most common), Kaolinite/Smectite, and Illite. They consist of either a 1:1 or 2:1 ratio of silica SiO_4 tetrahedrons to alumina AlO_6 octahedrons [59]. These nanoclays are naturally occurring and composed of 1-nm-thick aluminosilicate layers with cation exchange capacity (CEC) ranging from 80 to 120 meq/100g [95,96]. Higher CEC leads to dispersion and exfoliation of the

nanoclays [97] and, therefore, better interaction with the binder. Since asphalt is organophilic, surface modification of the clay is necessary to separate the silicate sheets and obtain a fine dispersion in the binder. In practice, Organo-Modified Montmorillonites (OMMT) are produced by adding quaternary ammonium salts with alkyl chains to MMTs. Studies have shown that the modification of asphalt with OMMT provides a stable mixture [60].

A study has shown that nanoclay modification is 22 to 33% cheaper than polymer modification, improving the binder's properties at a lower cost [11]. Interestingly, nanoclay-modification offered improved resistance to asphalt rutting [94] and fatigue [85]. It is reported that crack propagation is ceased through nanoclay-modification, as the nanoclay tends to move towards tips of the cracks driven by the high surface energy, hence blocking the increase of the cracks [98]. A study shows that compared to a control mixture, nanoclay modified asphalt mixtures have increased fatigue life cycles at high and intermediate temperatures but reduced fatigue life cycles at low temperatures [99]. Use of OMMT with concentrations of 2% to 4% has been shown to improve the work of cohesion and SFE of asphalt binders, as two significant indicators of self-healing capability [11]. Elsewhere, it was found that nanosilicates at 3% of the asphalt's weight can improve the healing ability of binders [65].

It is essential to highlight that while a binder healing test method has not been standardized to date, the most commonly used equipment to measure this phenomenon is known to be the Dynamic Shear Rheometer (DSR). A documented method for assessing the impact of healing on fatigue resistance due to the introduction of intermittent rest periods was developed; nonetheless, the effects of hardening were not considered [100]. Another recently developed approach to identifying asphalt's healing properties is based on imposed damage, using a DSR, which has shown relatively reliable results for neat binders [101]. As a simple indicator, a healing index was applied to identify the healing potential of asphalt binders based on a fatigue-rest fatigue method [102]. Further studies on self-healing led to an improved

methodology called the Two-Piece Healing (TPH) test and a framework to measure time-dependent healing due to SFE and the properties of the asphalt [5,49]. In the past, the TPH test has been used to assess healing in both aged and unaged binders. Using the TPH, the impact of rolling thin film oven (RTFO) and pressure ageing vessel (PAV) on the binder's rate of strength gain at different temperatures was evaluated [103]. At a lower rate than unaged binders, PAV aged binders showed a great capacity to heal after one hour rest period, with overall recovery reaching up to 68% at 20°C.

On the other hand, healing for RTFO-aged binder reached up to 96% at the same temperature [103]. Via employing the TPH test, it was observed that graphene oxide modification increases the intrinsic healing capacity of the binders, although long-term ageing showed an adverse effect on healing [75]. A study on the impact of the geometry of the samples during the TPH test noted that this procedure could produce reliable results provided that specimens are prepared to the best [104]. An investigation done on five different binders using the TPH test showed high repeatability [49].

4.2.1 Objectives and Scope

This research aims to investigate the self-healing properties of nanoclay-modified asphalt binder. For this purpose, two types of OMMT were high shear mixed with asphalt for this end. Samples were then collected from each asphalt binder and taken into a scanning electron microscope (SEM) to verify the proper dispersion of the nanosilicates into the binder's matrix. Next, standard Superpave tests were carried out on the binders to analyze the effects of nanoclay modification on their performance grading properties. In order to study the self-healing behaviour of both modified and non-modified asphalt binders, the TPH tests were also conducted using a DSR.

4.3 Materials

4.3.1 Nanoclays

Two types of OMMT were used here in this study, by which they were labelled as OMMT 1 and OMMT 2. The nanoclays in this research are commonly used for polymer modification [95,96]. The key properties of these materials are presented in Table 4-1.

Table 4-1. Physical properties of the Nanoclays [95,96]

Property (unit)	OMMT 1	OMMT 2
Organic Modifier	dimethyl dihydrogenated tallow	dimethyl dihydrogenated tallow
Modifier Concentration (meq/100g of clay)	125	95
Specific gravity (g/cc)	1.66	1.77
X-Ray Diffraction d-spacing (Å)	31.5	31.5

4.3.2 Asphalt Binder

All the supplied binders used in this research were produced from the same crude oil source. An asphalt with high-performance grading (PG) of 64°C, intermediate PG of 13°C, and low PG of -28°C was used as the control samples. The nanoclay-modified asphalts were produced by modifying the same binder at different dosages. Table 4-2 shows a summary of the control binder's physical properties.

Table 4-2. Control Binder Physical and Chemical Properties [105]

Component	Description
Performance Grade	PG 64-28
Penetration Grade	120/150
Physical state	Liquid
Melting Point / Freezing	> 31°C
Boiling Range	> 228°C (1 atm)
Flash Point	> 243°C (COC)
Density	> 1 kg/L at 15°C
Relative Density	1.020 – 1.040 (Water = 1) at 15°C (1 atm)

*COC = Cleveland open cup

4.3.3 Modification Method

Previous studies have shown that using a high shear mixer at a high temperature provides a well-mixed structure [84,90,93]. In particular, using 3000 rotations per minute (RPM) at 130 °C for 2 hours has provided good mixtures [84]. A similar protocol was followed in the current study by placing the binder container over a hot plate to maintain the binder temperature at 130 ± 2 °C. At the same time, a thermometer was kept in the container to invigilate it. A total of five different binders were studied: unmodified binder (PG 64-28), PG 64-28 + 2% OMMT 1, PG 64-28 + 4% OMMT 1, PG 64-28 + 2% OMMT 2 and PG 64-28 + 4% OMMT 2. Initially, the nanoclays were poured in the heated asphalt binder followed by mechanically mixing for 5 minutes to provide submersion of the clays. The high shear mixer was set to 3000 RPM for 2 hours.

4.4 Testing Program

4.4.1 Scanning Electron Microscope

Adequate dispersion of nanoclays in the binder is of utmost importance to ensure efficient modification. Considering this fact, an SEM, a Zeiss Gemini 500 Field Emission Scanning Electron Microscope, capable of providing images at the nanoscale with magnifications from 50x to 2,000,000x the samples' scope used to investigate the dispersion of the nanomodified binders. To do so, thin layers of asphalt were spread onto SEM pin mounts. These samples were taken to gold coating equipment, where they sputtered with gold to identify the nanoclays on the matrix. The SEM magnified the specimen from 500x to 20,000x, where an analysis of the dispersion was done.

4.4.2 Performance Grading

Superpave performance grading was performed following AASHTO M 320-17 to characterize all binders [25]. The PG grading aimed to analyze the impact of nanoclays on the overall performance of binders. Consequently, high PG was investigated on all unaged modified and neat binders using a DSR. Besides, binders were also RTFO-aged according to AASHTO T 240-

13 short-term aged properties [21]. Samples were also PAV-aged according to AASHTO R 28-12 targeting intermediate temperature grading using a DSR [22]. Finally, the bending beam rheometer (BBR) was employed to test the low-temperature PG according to AASHTO T 313-12 [26].

4.4.3 Two-Piece Healing Test

The TPH test measures the binder's ability to recover its complex shear modulus (G*) after experiencing the fatigue cracking. An intrinsic healing function $R_h(t)$ represented in equation (4-1) is calculated and expressed in percentage repressing the expected healing at time = t. It should be noted here that healing occurs in two phases: instantaneous healing, which is caused by wetting of the cracked surfaces, and interfacial cohesion, which is represented as R_0 in equation (4-1). Due to the infeasibility of measuring the G* at time = 0, R_0 is defined by the first reading, at t = 1 minute. The other healing phase is the over-time healing, caused by interdiffusion and randomization of molecules, which is represented by the second part of equation (4-1): $p(1 - e^{-qt^r})$ [5].

$$R_h(t) = R_0 + p(1 - e^{-qt^r}) \quad (4\text{-}1)$$

where:

R_h = intrinsic healing

t = time in minutes

R_0 = ratio healed at 1 minute

p = ratio left to be healed at 1 minutes

q = asphalt property

r = asphalt property

It is worth mentioning that Equation (4-1) is a modified version of Avrami's equation, which is a model used to describe chemical reactions [5]. The original framework developed for the

TPH test was difficult to obtain the unknown parameters: p, q, and r. Further development of the framework led to improvements in parameter p definition and the calculation of the parameters q and r. The second part of equation (4-1) is the over-time healing, and an infinite time, the healing percentage of asphalt is expected to be 100%. The parameter p was then redefined as equal 100 – R_0 [49].

For this test, three silicon moulds were prepared, including one mould with cavity dimensions of 18-mm and height of 7-mm and two moulds with cavity dimensions of 18-mm and height of 3.5-mm. The test protocol consisted of one-piece and two-piece tests.

4.4.3.1 One-Piece Testing Procedure

The one-piece portion of the test represents a control sample, meaning a piece that has not been damaged by cracking. An unaged asphalt binder was heated in an oven at 130 °C for 30 minutes and then poured into the silicone mould with a diameter of 18-mm and thickness of 7-mm. A DSR with a 25-mm diameter spindle was used to measure the G* of the binder, by which its 25-mm diameter base plate is pre-heated to 25 °C. The test configuration was set to minimize interference of the equipment in the healing process of the binders. The frequency was set at 10 rad/s, maintaining a constant strain amplitude of 0.001 % and normal force of 0.4 N. The samples were subject to 30-minute rest periods after being prepared for conditioning at room temperature. The specimen was then detached from the mould and measured to ensure the height was within 7 ± 0.5 mm and then attached to the center of the DSR's base plate. The gap between the spindle and the base plate was then reduced to 5-mm. The G* of the binder was measured at 1, 3, 5, 7, 10, 15, 20, 27, 37, 47, and 57-minute intervals. Due to the sensitivity of this test, the procedure was repeated six times to ensure consistent results.

4.4.3.2 Two-Piece Testing Procedure

The two-piece portion of the test represents an asphalt sample that has gone through a full crack, and it has been allowed to rest and heal with minimum intervention while the cracked

surfaces are entirely in contact. The same unaged binder used to obtain the one-piece portion is heated in an oven at 130 °C for 30 minutes and then poured into two silicon moulds with dimensions of 18-mm diameter and 3.5-mm thickness. The configurations of the DSR are identical to the one-piece portion to minimize the influence of the testing procedure on the results. The samples were also given 30-minute rest periods after being prepared for conditioning at room temperature. The specimen was then detached from the mould and measured to ensure the height was within 3.5± 0.5 mm. One of the specimens was attached to the base plate, while the other was attached to the bottom of the spindle. It was ensured that the samples were centred, and the gap between the spindle and the base plate was then reduced to 5-mm. The complex shear modulus of the binder was measured at 1, 3, 5, 7, 10, 15, 20, 27, 37, 47, and 57-minutes.

Similarly, due to the sensitivity of this test, the procedure is repeated six times to ensure consistent results. Figure 4-1 displays the steps taken using DSR for the two-piece healing test procedure. At part (a), the 7-mm specimen is well-centred on the bottom portion of the spindle and at part (b), the gap between the spindle and the base plate is reduced to 5-mm, both representing the steps in the one-piece portion. At part (c), the binders are well-centred on the base plate and the spindle and part (d), the gap between the spindle and the base plate is reduced to 5-mm, both representing the steps in the two-piece portion.

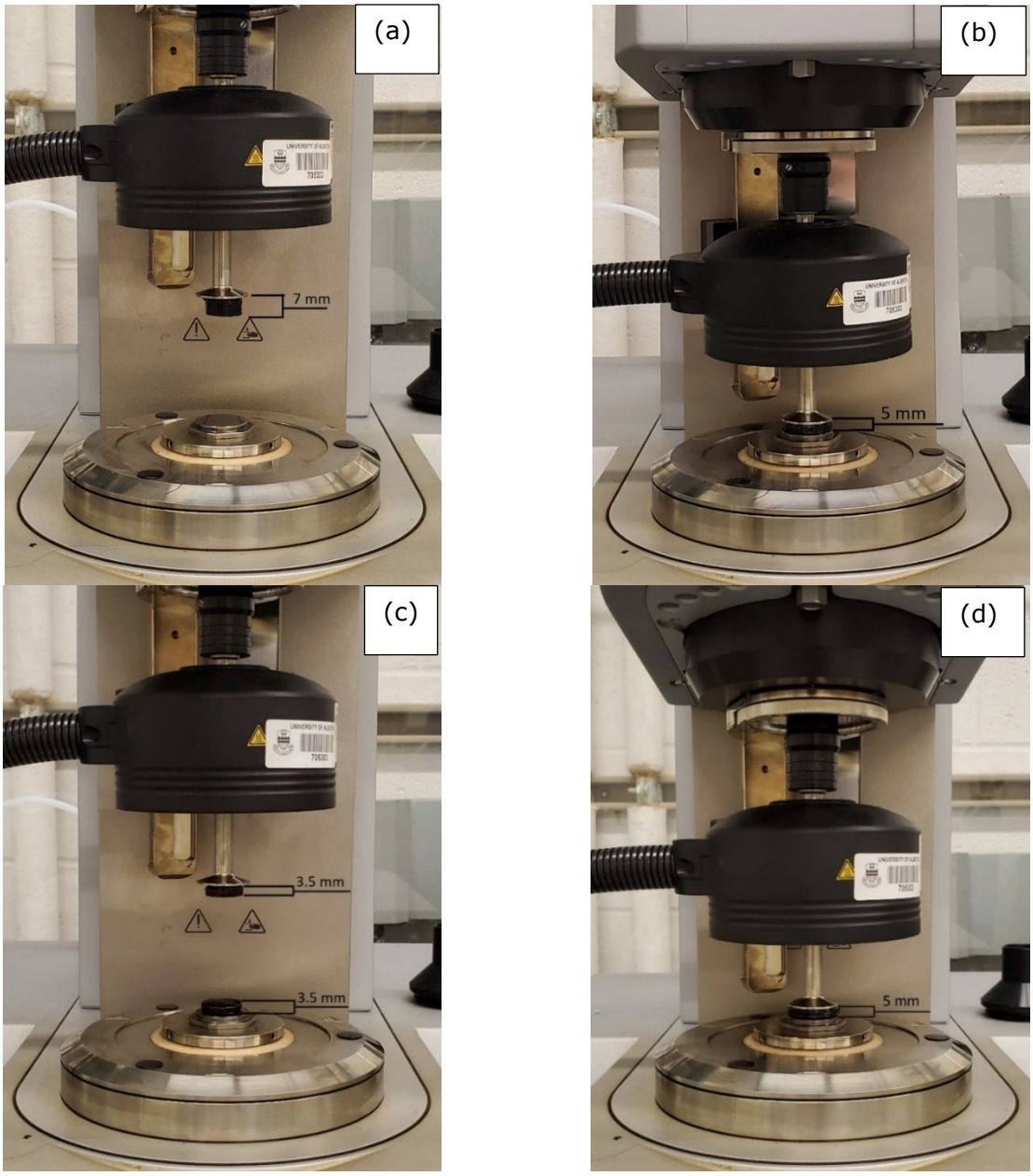

Figure 4-1. a) one-piece sample before gap reduction, b) one-piece sample with gap at 5-mm, c) two-piece sample before gap reduction, d) two-piece sample with gap at 5-mm

4.4.3.3 Intrinsic Healing Function Calculation

The obtained results from both parts were utilized to calculate the healing percentage (H%), represented by equation (4-2) [49].

$$H\%(t) = \frac{G^*(t)\ two-piece}{G^*(t)\ one-piece} x\ 100 \qquad (4\text{-}2)$$

where:

H% = healing percentage

G* = Complex Shear Modulus

t = time in minutes

Averages of the G* obtained from one-piece and two-piece were used to calculate H%(t). At time = 1 minute, the healing percentage represents the instantaneous healing in the intrinsic healing function, R_0. The parameter p is calculated as 100 - R_0, while parameter r and parameter q are obtained from a minimum squared error of equation (4-1) based on equation (4-2). After the parameter was found, intrinsic healing parameters were found, Rh can be estimated for any time (t) for the binder analyzed. The parameter q was defined as a temperature-dependent constant, while r is a material constant representing the rate of internal transformation while comparing aged binders [103]. According to the literature, SFE is the driving force on wetting and, therefore, R_0 [49].

4.5 Results And Discussion

4.5.1 Dispersion

A qualitative analysis of the dispersion of nanoclays was made based on SEM images. The samples were magnified to a scope ranging from 500x to 20,000x. Samples collected for the SEM were chosen for the binders with the higher concentration of nanoclay at 4% dosage, which presumably presents reduced dispersion compared to the 2% dosage, as it would lead to higher agglomerations. Figure 4-2 shows the images of the nanoclay-modified asphalt at a magnification of 5,000x. Figure 4-2 (a) is an image of the modified asphalt binder with 4% OMMT 1, in good dispersion of the nanoclay with very few agglomerations was noticed. Figure 4-2 (b) presents an image of the asphalt binder modified with 4% OMMT 2, in which the agglomerations were slightly larger and nanoclays were well dispersed in the binder.

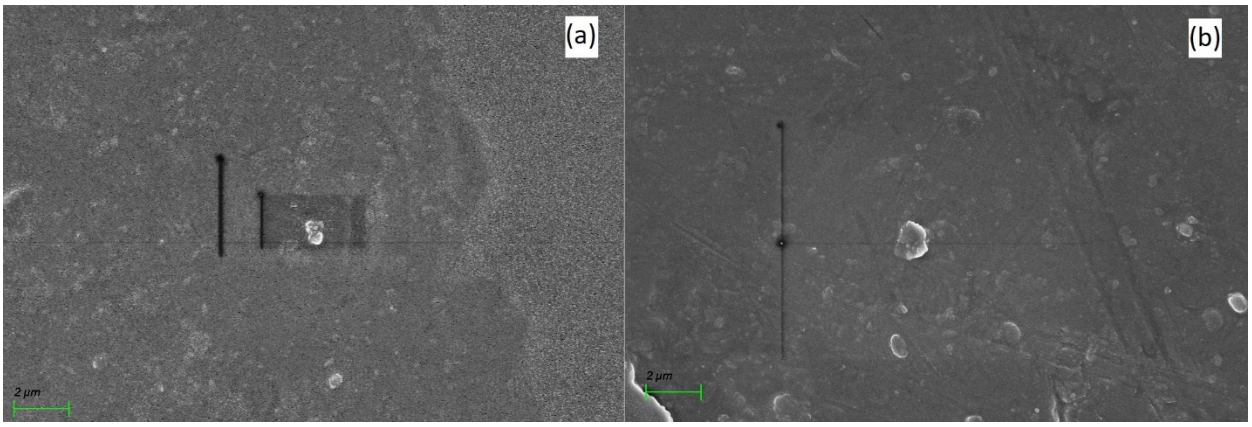

Figure 4-2. SEM images (a) 4% OMMT 1, (b) 4% OMMT 2

4.5.2 Performance Grading Results

The asphalt binders were tested for the high, intermediate, and low PG grades. Table 4-3 summarizes the results obtained for each of the asphalt binders. An increase in high-temperature performance was observed in all OMMT modified binders. It was found that the higher concentration of nanoclays presented more elevated values. Both OMMTs showed similar improvement trends in the high PG grade. As previously mentioned, low-temperature PG grade was also evaluated using BBR. Results showed that the addition of OMMT 1 and OMMT 2 presented no significant change in the lower temperature performance of the asphalt binders. Eventually, intermediate temperature PG grades increased by adding OMMT 2; however, no differences were noticed for OMMT 1 at 4%.

Table 4-3. Performance grading of modified and non-modified binders

Asphalt Binder	True Unaged High PG	True RTFO High PG	True Low Temperature (°C) @ 300 MPa	True Low Temperature (°C) @ m_value of .300	Intermediate PG Grade
PG 64-28	64.2	65.3	−20.6	−22.0	12.6
PG 64-28 + 2% OMMT 1	66.6	67.3	−20.6	−22.9	13.7
PG 64-28 + 4% OMMT 1	70.6	70.0	−20.6	−22.8	12.8
PG 64-28 + 2% OMMT 2	67.9	67.0	−20.3	−22.6	15.0
PG 64-28 + 4% OMMT 2	70.0	70.2	−19.8	−21.7	17.2

4.5.3 Two-Piece Healing Test

4.5.3.1 Complex Shear Modulus

The G* of the asphalt binders was measured according to the TPH test procedure, and Table 4-4 displays the binders' G* at specific times. It is possible to see that the two-piece results were much lower at initial readings than the one-piece results, but the differences between them were reduced over time. It was observed that the modified binders had higher G* values compared to the PG 64-28 binder and that higher dosages of nanoclay provided higher G*. An example of this increase can be seen comparing initial readings of one-piece, where G* were 88.6 MPa for PG 64-28 binder, 108.0 MPa for 2% OMMT 2 and 163.0 for 4% OMMT 2.

Table 4-4. TPH test Complex Shear Modulus

Elapsed Time (min)	PG 64-28 Binder (MPa)		PG 64-28 Binder + 2% OMMT 1 (MPa)		PG 64-28 Binder + 4% OMMT 1 (MPa)		PG 64-28 Binder + 2% OMMT 2 (MPa)		PG 64-28 Binder + 4% OMMT 2 (MPa)	
	One-Piece	Two-Piece	One-Piece	Two-Piece	One-Piece	Two-Piece	One-Piece	Two-Piece	One-Piece	Two-Piece
1	88.6	57.7	88.9	65.0	109.0	97.5	108.0	84.4	163.0	140.0
3	83.1	57.1	91.8	76.5	123.0	106.0	122.0	95.5	174.0	151.0
5	88.2	59.8	103.0	80.1	128.0	114.0	126.0	106.0	184.0	163.0
7	94.6	62.5	111.0	87.0	136.0	127.0	131.0	114.0	160.0	146.0
10	97.9	75.7	111.0	93.9	145.0	129.0	130.0	124.0	164.0	148.0
15	108.0	76.0	126.0	106.0	153.0	143.0	145.0	121.0	169.0	153.0
20	110.0	79.1	133.0	109.0	154.0	149.0	146.0	123.0	164.0	153.0
27	111.0	79.2	136.0	113.0	167.0	153.0	145.0	132.0	162.0	149.0
37	114.0	84.3	139.0	116.0	165.0	158.0	149.0	130.0	167.0	158.0
47	117.0	90.9	136.0	117.0	172.0	158.0	155.0	125.0	184.0	163.0
57	114.0	94.9	139.0	123.0	168.0	162.0	154.0	132.0	175.0	165.0

Figure 4-3 (a) and (b) show the percentage of G* gained by the nanoclay-modified binders for one-piece and two-piece samples, respectively, compared to the neat binder. According to these figures, the increase in initial modulus became more stable following the first 10 minutes. With that, an average percentage increase was calculated for the values from 10

minutes to 57 minutes. The gains of G* percentage under one-piece test were 20% for 2% OMMT 1, 46% for 4% OMMT 1, 33% for 2% OMMT 2 and 54% for 4% OMMT 2. The increases in percentage of G* under two-piece were 37% for 2% OMMT 1, 82% for 4% OMMT 1, 54% for 2% OMMT 2 and 88% for 4% OMMT 2. These values indicate that the nanoclay-modification led to a pronounced impact on the two-piece specimen.

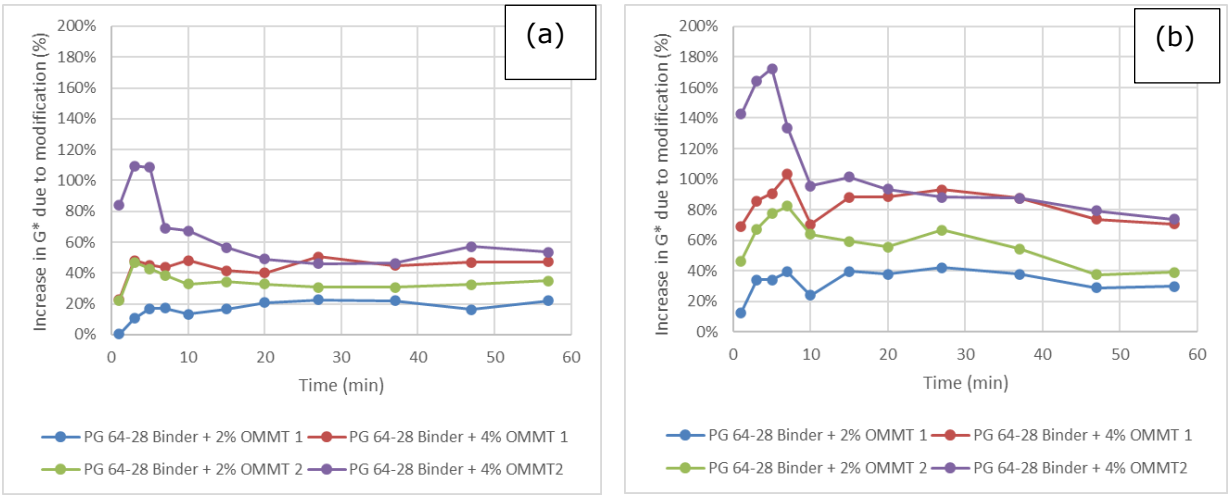

Figure 4-3. (a) G* ratio increase of nanoclay-modified binder to neat binder from one-piece test, (b) G* ratio increase of nanoclay-modified binder to neat binder from two-piece test

Average ratios of G* presented by the nanoclay-modified binder over neat binder were calculated for both one-piece and two-piece tests. The average values were based on results from 10 to 57 minutes of readings. Bar charts presented in Figure 4-4 represent the calculated ratios in all cases. It is visible that the addition of the nanoclays in both concentration levels led to higher G* of the binders, with the minimum G* ratio of modified binders to neat binders value being 1.20. It is also visible that the impact of nanoclays was more significant in the case of the two-piece samples, meaning that with healing, the nanoclay-modified binder possessed much higher G* than a neat binder. OMMT 1 and OMMT 2 at 4% concentrations resulted in higher G* of the binders compared to 2% concentration. The G* ratio of 4% OMMT 1 binder to the neat binder for the two-piece samples is 1.88, indicating a much higher G* for the modified binder.

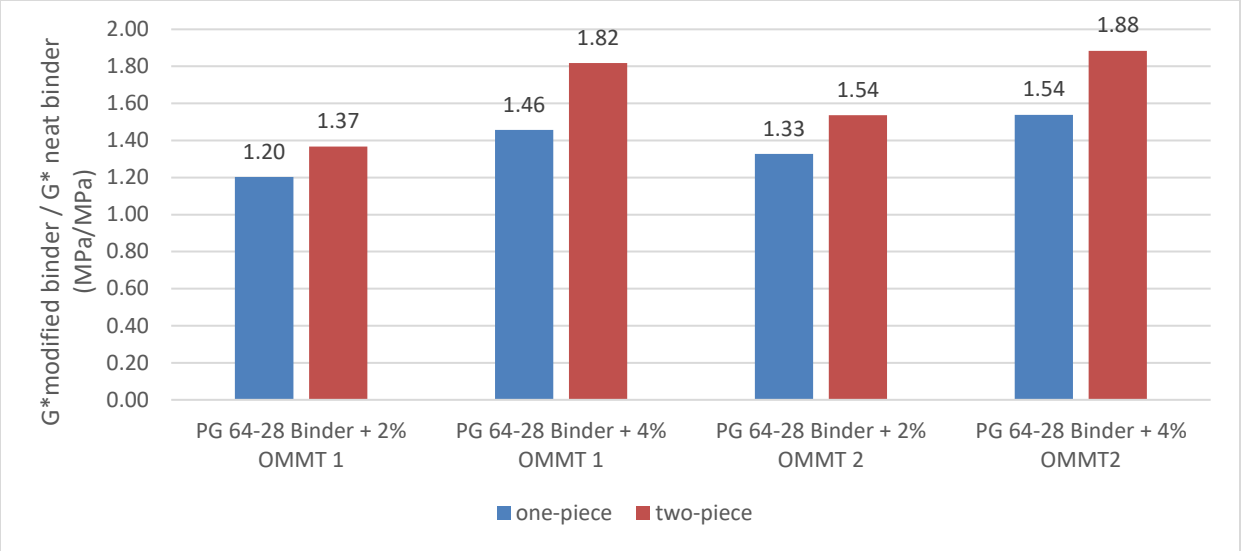

Figure 4-4. Average ratio of G* presented by nanoclay-modified binders over neat binders

4.5.3.2 Self-Healing Results and Discussion

The binders' intrinsic healing functions were calculated using the values obtained from Table 4-4 and the healing percentage formula presented in equation (4-2). The parameters obtained from equation (4-1) are displayed in Table 4-5. Based on the calculated R_0 values, which show the portion of healing during wetting, the modified binders performed significantly better instantly after the cracked surfaces came in full contact, which is as expected, as nanoclay modified binders have higher SFE [11]. OMMT 1 and OMMT 2 showed similar trends in improving the instant healing of asphalt. The binders made with 4% OMMT 1 and 4% OMMT 2 had R_0 equal 90% and 86%, respectively. The parameter R_0, which is closely related to SFE, indicated higher SFE with modification.

Table 4-5. Intrinsic Healing Function Parameters

Parameter	PG 64-28 Binder	PG 64-28 Binder + 2% OMMT 1	PG 64-28 Binder + 4% OMMT 1	PG 64-28 Binder + 2% OMMT 2	PG 64-28 Binder + 4% OMMT 2
R_0	0.651	0.732	0.897	0.780	0.860
p	0.349	0.268	0.103	0.220	0.140
q	0.033	0.211	0.032	0.317	0.146
r	0.690	0.307	0.815	0.110	0.404

R_h for each of the modified binders was plotted and presented in Figure 4-5. The trend shows that 4% OMMT 1 followed by 4% OMMT 2 depicted the highest properties recovery after 56 minutes at 96% and 93%, respectively. The binders modified with 2% OMMT 1 and 2% OMMT 2 also had higher recovery rates than the unmodified binder, with both of them presenting 87% healing percentages at 57 minutes against 79% for the PG 64-28 binder.

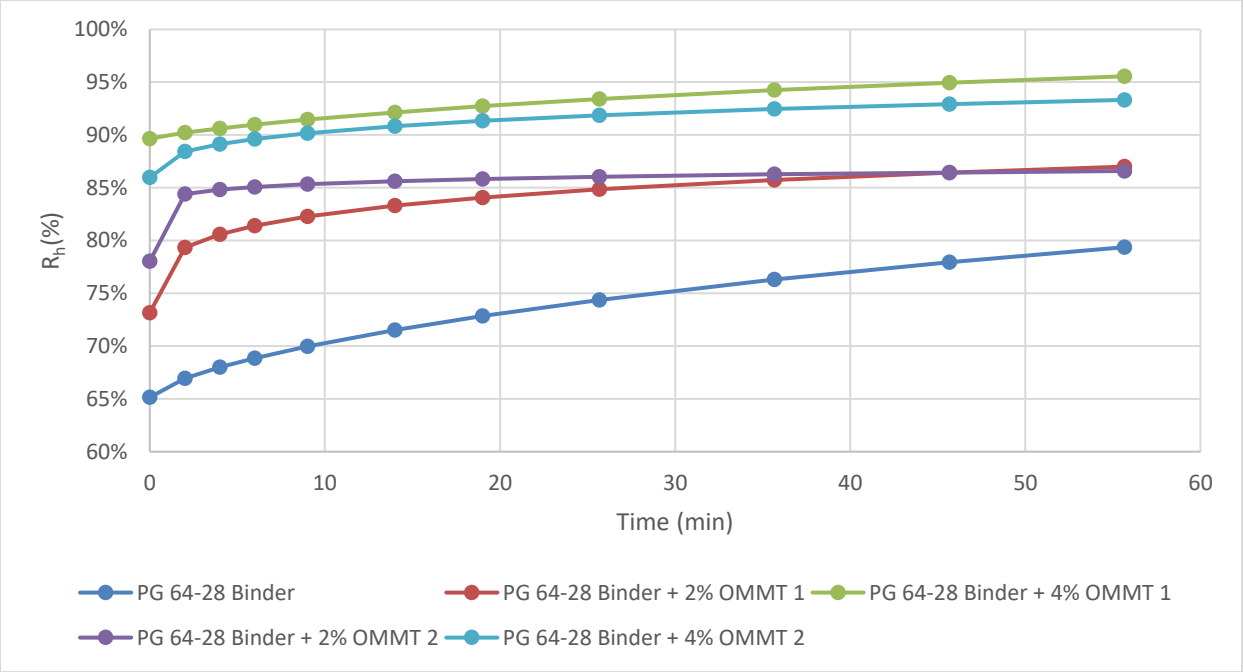

Figure 4-5. Intrinsic Healing Percentage of Nanoclay-Modified Binders

Overall, the nanoclays improved the healing ability of the asphalt binders. Figure 4-6 (a), divides the healing into instantaneous healing, overtime time healing, and total healing. The OMMT 1 and OMMT 2 at 4% concentration showed high overall properties recovery with 96% and 93%, respectively, having nearly the same properties as before cracking. The PG 64-28 binder and the 2% OMMT 1 modified binder presented the highest overtime healing ratios at 14%, but they also had the lowest R_0s at 65% and 73%, respectively. Results corresponding to OMMT at each concentration are shown in Figure 4-6 (b). The nanoclays at 4% dosage exhibited the most significant improvements, with OMMT 1 improving 9% of the high PG grade and 38% of the instantaneous healing compared to the PG 64-28 asphalt binder. OMMT 2 at

4% concentration also improved the performance of the binder with increases of 9% for high PG grade and 32% instantaneous healing.

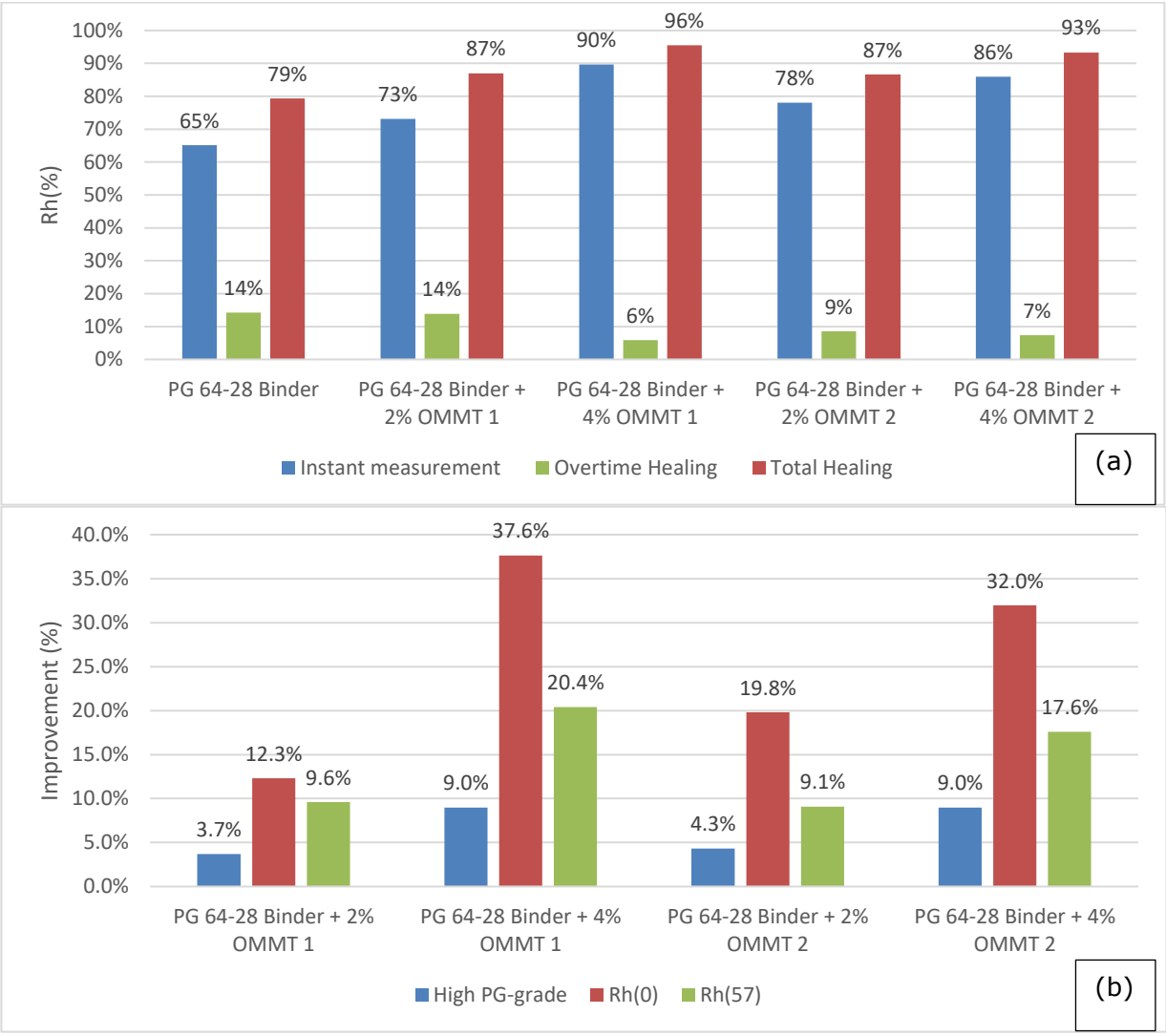

Figure 4-6. Comparison between (a) constant healing and overtime healing, (b) improvements in OMMT-modified binders

4.6 Conclusions

This study investigated the change in G* and the intrinsic healing properties of nanoclay-modified asphalt binders. The testing and analysis of this work led to the following conclusions:

- The qualitative analysis based on the SEM demonstrated that the high shear mixer procedure used presented a well-dispersed mixture of nanoclay in the matrix.
- Improvements were observed for all concentrations of nanoclay, with the 4 % OMMT 1 and the 4% OMMT 2 binders presenting 9% increases in high-temperature performance properties.
- OMMT 1 and OMMT 2 modifications did not impact the low-temperature performance of the asphalt binder.
- The increase in G* by nanoclay-modification was more significant on the two-piece samples. The G* ratio between modified binders and neat binders ranged from 1.20 to 1.88.
- The binder modified with 4% OMMT 1 showed the highest instant healing with 90%, while the neat and the 2% OMMT 1 were significantly impacted by rest periods with increases of 14% in G* over 56 minutes period.
- Compared with the PG 64-28 binder, improvements in the instantaneous healing of asphalt were found to be 37% for 4% OMMT 1 and 32% for 4% OMMT 2.
- The introduction of a rest period of 56 minutes led to nearly complete recovery of the properties (around 96% of original G*) for 4% OMMT 1 modified binder
- The results obtained from this study show that OMMT 1 and OMMT 2 at both 2% and 4% concentration improved the overall healing of the binder and therefore have great potential to increase the service life of asphalt pavements.

5 Investigation of Laboratory Aging Effects on Nanoclay-Modified Asphalt Binders

5.1 Abstract

Asphalt binder ageing is a complex phenomenon that plays an essential role in reducing flexible pavement serviceability. Thus, this work investigated the impact of montmorillonite nanoclays on the asphalt's ageing resistance, storage stability, performance grading, and rutting resistance. In this study, laboratory ageing was carried out for asphalt binders containing two types of nanoclays of 2% and 4% weight. The binders were subjected to Rolling Thin-Film Oven and Pressure Aging Vessel, followed by rheological analysis employing a Dynamic Shear Rheometer and a Bending Beam Rheometer. Differences in the ageing behaviour of tested binders were noted based on the developed master curves and ageing indices. The results showed improved ageing resistance in the case of montmorillonite nanoclay modified asphalts.

5.2 Introduction

Asphalt binder ageing is one of the main issues that cause different forms of distresses in the pavement. As the binder ages, there are two ageing asphalt forms: the first form, short-term ageing, occurs during the construction phase. Short-term ageing is a result of binder volatilization and reduction of oil constituents. The second form, long-term ageing, occurs during the pavement life cycle due to weathering and oxidation. Dependent on asphalt mixture composition, long-term ageing results from oxidation, polymerization, and photo-oxidation of surface layers. [106]. Usually, ageing due to the effect of heat and air at the mixing and compaction stage can be simulated employing the Rolling Thin-Film Oven (RTFO) test [21]. On the other hand, the impact of oxidation during 5 to 10 years of asphalt pavement service life is simulated using the Pressure Aging Vessel (PAV) test [22]. Asphalt is a viscoelastic material; its mechanical properties depend on time, temperature, and strain [107]. Therefore, the properties commonly used to describe RTFO-aged and PAV-aged asphalt binders, being the complex shear modulus (G*) and the phase angle (δ), are characterized at different

loading times (frequencies) and temperatures via a Dynamic Shear Rheometer (DSR). It is known that due to the viscoelastic behaviour of asphalt, rheological measurement can be challenging under very low- or very high temperatures and frequencies [108].

The leading solution to address ageing in asphalt is modifying the asphalt binder to improve rheological properties and antiaging performance [109]. Binder modification is an emerging trend of asphalt. Studies through the past decade have reported that adding materials such as resins, rubbers, polymers, sulphur, fibres, clays, and powders lead to improvements in rutting resistance, ageing resistance, low-temperature cracking, and increase of fatigue life [99,110–112]. Nanomaterials have the potential of improving asphalt properties from on the nanoscale dimension due to their morphology [113]. Although many mechanical properties are improved, some of these modifications come with setbacks. For example, several studies have found that Styrene-Butadiene-Styrene (SBS) modified binder has poor ageing resistance, poor storage stability, and elevates the cost of construction [12,13,84]. Contrarily, nanoclay modification is 22-33% cheaper than SBS and may lead to improved ageing resistance, as the layered silicates in nanoclay block asphalt oxidation [16,84]. Furthermore, a study showed that Organo-Montmorillonite (OMMT)-modified asphalt binder exhibited improved rheological properties such as higher penetration grade and lower ageing index when compared to non-modified [16]. In light of the reported rheological improvements and potential improvements in ageing resistance by adding OMMT to asphalt, for this study, two types of OMMT were used to modify asphalt binders.

This work aims to investigate and compare the properties of neat and nanoclay-modified asphalt binders under short- and long-term ageing through master curves and ageing indices. Also, by examining the evolution of saturates, asphaltenes, resins, and aromatics (SARA) fractions, the current study aims to analyze the storage stability of nanoclay modified binders and composition related to ageing. Additionally, this study evaluates the dispersion of OMMT and the performance grading of OMMT modified binders.

5.3 Experimental Study

5.3.1 Materials

Nanoclays are made up of clays with at least one of their dimensions on the nanoscale. These clays can be classified into four groups: Illite, Chlorite, Kaolinite, and Montmorillonite (MMT) [59]. This last one is the most widely used polymer modifier [15]. MMTs are naturally hydrophilic silicates composed of a 2:1 tetrahedral-to-octahedral layer arrangement [14]. Surface-modified MMTs, called OMMTs, disperse into intercalated and exfoliated structures in the asphalt base, while MMTs are not compatible with asphalt [114].

This study used five asphalt binders, including unmodified and four nanoclay-modified binders. The neat PG 64-28 with an intermediate grade of 13°C, a boiling range of at least 228°C, and a flashpoint of at least 243°C were modified by two OMMTs referred to after this as OMMT 1 and OMMT 2.

The nanoclay-modified asphalt binders were prepared using a High Shear Mixer (HSM) at 130 ± 2°C for two hours at 3,000 rotations per minute. This study used two different dosages of each nanoclay: 2% OMMT 1, 4% OMMT 1, 2% OMMT 2, and 4% OMMT 2 by weight of asphalt binder.

5.3.2 Scanning Electron Microscope

The dispersion of the nanomaterials through the matrix of the asphalt binder is essential for rheological and mechanical improvements. For this reason, a Zeiss Geminin 500 Field Emission Scanning Electron Microscope (FE-SEM) was employed to obtain a qualitative analysis of the nanoclay dispersion for the chosen mixing method. Nanoclay modified asphalt binder samples were attached on FE-SEM pin mounts and observed under the scope of 500 x to 20000 x. From the images obtained, the dispersion of the OMMTs resulting from mixing was visually analyzed.

5.3.3 SARA Fraction Analysis

Asphalt binder comprises four fractions: saturates, aromatics, resins, and asphaltenes (SARA), correlated to its properties [90]. The SARA analysis method used in this study is the gravity-driven chromatographic separation of saturates, resins, and aromatic fractions. The asphaltenes are first separated from the sample by mixing the binder with heptane, then heated under reflux according to the ASTM D6560 [115]. The saturates, aromatics, and resins are determined by the clay-gel adsorption chromatography method by following the ASTM D2007 [116]. Due to the colloidal nature of asphalt, the SARA fractions can be used to calculate its storage stability [117]. Thus, the results were used to calculate Colloidal Indices (CI) as shown in equation (5-1) [118].

$$CI = Saturates + Asphaltenes/Resins + Aromatics \quad (5\text{-}1)$$

According to the literature, CI values higher than 0.9 indicate a stiff and unstable binder, while values below 0.7 indicate a very stable and soft material [117,118]. Therefore, a storage-stable asphalt has a CI below 0.9 but not much lower than 0.7, so it can resist rutting.

5.3.4 Laboratory Aging Procedures

The five types of binder used in this study were aged for 85 minutes at 163°C in an RTFO oven according to AASHTO T 240-13 [21]. These RTFO-aged binders were further investigated and used for PAV ageing for 20 hr, under 2.1 MPa pressure at 100ºC, according to AASHTO R 28-12 [22].

5.3.5 Asphalt Binder Performance Grading

The impact of the nanoclays on the PG grade of the asphalt binders was investigated according to AASHTO M 320 [25]. The high-temperature grades of the binders were determined by employing an Anton Paar SmartPave 102 DSR on unaged and RTFO aged binders. Additionally, the low-temperature grades of the asphalt binders were obtained on the PAV-aged samples using a Bending Beam Rheometer (BBR) according to AASHTO T 313-12 [26].

5.3.6 Asphalt Binder Frequency-Sweep Test

The frequency sweep (FS) test is an advantageous method to evaluate the viscoelastic properties of asphalt binders. Due to the difficulty of testing asphalt binders under extreme conditions, G* and δ master curves were constructed using time-temperatures superpositions (TTSP) for asphalt materials. Through creating master curves, i.e., horizontally shifting various FS results under a reference temperature, one can characterize the rheological properties of the binder at a broader range of frequencies [108,119,120]. This study conducted an FS test at the frequency range of 0.01 to 100 rad/s and five different temperatures (10, 20, 25, 30, and 40ºC) on the aged and unaged binders. The DSR was configured under a setting to test samples with 8-mm diameter, 2-mm gap, 1% shear strain under the linear viscoelastic range. These frequency-sweep settings were appropriate to evaluate the rheological, fatigue, and relaxation properties of aged and unaged binders [121,122].

The TTSP method was applied via shifting FS functions of G* and δ determined under various temperatures to a reference temperature of 25ºC [108,118]. A study has shown that 25ºC is appropriate for investigating fatigue behaviour of asphalt binders [123].

Two ageing indices, namely complex modulus ageing index (CAI) represented by equation (5-2) and phase angle ageing index (PAI), defined by equation (5-3), were determined in this analysis. Mainly, high CAI values indicate a high ageing degree, while high PAI values indicate a low ageing degree [112]

$$CAI = Aged\ Complex\ Modulus / Unaged\ Complex\ Modulus \quad (5\text{-}2)$$

$$PAI = Aged\ Phase\ Angle / Unaged\ Phase\ Angle \quad (5\text{-}3)$$

5.4 Results and Discussion

5.4.1 Dispersion and Stability Results

Figure 5-1 (a) shows well-dispersed OMMT 1 at 4% concentration into the asphalt binder. The circles indicate places with agglomerations, and as seen, there were few agglomerations with dimensions smaller than 2 μm. The binder with 4% OMMT 2 was also analyzed for dispersion, as seen in Figure 5-1 (b). Both OMMT 1 and OMMT 2 have similar structures, with the difference being in their concentration of surface modifiers. Although similar, the asphalt binder with 4% OMMT 2 showed slightly lower interaction with the binder, with more agglomerations throughout the matrix. However, this mixture also seemed to be well-dispersed, having very spaced nanoclay clusters with proportions smaller than 2 μm.

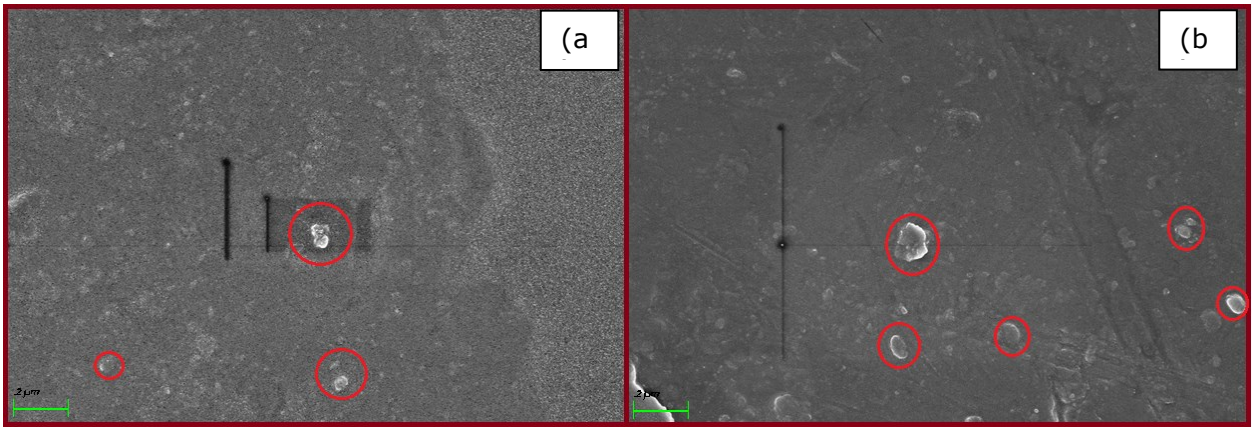

Figure 5-1. SEM magnifications of binder modified with: (a) 4% OMMT 1, (b) 4% OMMT 2

In order to quantify the storage stability of the modified binders, the CI was calculated based on SARA results. Table 1 shows the results obtained from SARA and CI. The fraction regarding the asphaltenes, which is an essential indicator of the binder stiffness, was lower in the modified asphalt binders. Higher concentrations of nanoclays decreased the fractions of asphaltenes to 15.49% and 16.31%, for 4% OMMT 1 and 4% OMMT 2, respectively, from 21.09% in non-modified asphalt binder. The opposite behaviour was observed regarding the Saturates and Resins, as they increased with the addition of the nanoclays. A study indicates that the Saturates fraction is the prominent indicator of the rheological properties in asphalt

binders, and its increase indicates lower G* and higher δ [118]. The results obtained from the CI calculation, as seen in Table 5-1, suggest that the addition of the nanoclays increases the storage stability. Specimens with 4% OMMT 1 and 4% OMMT 2 showed to be more stable with CI at 0.76 and 0.81, respectively, compared to 0.88 of the non-modified binder. They were found to be stable but stiff enough to resist rutting. The addition of 2% OMMT 1 and OMMT 2 provided stability to the binders with CI below 0.88 resulting from the neat binder.

Table 5-1. SARA and CI results

Sample	Saturates (%)	Asphaltenes (%)	Resins (%)	Aromatics (%)	CI
PG 64-28	25.58	21.13	32.22	21.07	0.88
PG 64-28 + 2% OMMT 1	26.42	18.73	33.23	21.62	0.82
PG 64-28 + 4% OMMT 1	27.38	15.67	34.09	22.87	0.76
PG 64-28 + 2% OMMT 2	26.82	17.22	36.73	19.24	0.79
PG 64-28 + 4% OMMT 2	28.32	16.50	36.63	18.55	0.81

5.4.2 Performance Grading (PG) Results

Binder modification affects various properties of the asphalt binder, and their impacts on workability, permanent deformation, fatigue cracking, and low-temperature cracking were investigated by performing the Superpave Performance Grading, and the results are presented in Table 5-2. Initially, the high-temperature PG grade of unaged samples indicated improvements due to binder modification. The actual high-temperature PG grade was equal to 64.2 for the unmodified binder, which increased to 70.6 and 70.0 after 4% OMMT 1 and 4% OMMT 2 modifications, respectively. At lower dosage (2%), the actual unaged high PG grade increased to 66.6 and 67.9 for OMMT 1 and OMMT 2, respectively. Following RTFO ageing, the same increasing trend was noticed by which the actual high PG grade of 65.3 for the unmodified sample increased to 67.3, 67.0, 70.0, and 70.2 for 2% OMMT 1, 2% OMMT 2, 4% OMMT 1, and 4% OMMT 2, respectively. The BBR testing of PAV-aged samples indicated that the OMMTs had no significant impact on the critical temperature corresponding to

maximum creep stiffness of 300 MPa and m-value of 0.300. Overall, the PGs were found to be 70-28 for OMMT 1 and OMMT 2, both at 4% nanoclay concentration.

Table 5-2. Performance Grading results

Sample	True Unaged High PG	True RTFO High PG	True Low Temperature (°C) @ 300 MPa	True Low Temperature (°C) @ m_value of .300	PG-Grade
PG 64-28	64.2	65.3	−20.6	−22.0	64-28
PG 64-28 + 2% OMMT 1	66.6	67.3	−20.6	−22.9	64-28
PG 64-28 + 4% OMMT 1	70.6	70.0	−20.6	−22.8	70-28
PG 64-28 + 2% OMMT 2	67.9	67.0	−20.3	−22.6	64-28
PG 64-28 + 4% OMMT 2	70.0	70.2	−19.8	−21.7	70-28

5.4.3 Frequency Sweep Test Results

To study the ageing behaviour of nanoclay modified binders, FS tests were conducted on the neat and modified asphalt binders under unaged, RTFO-aged, and PAV-aged conditions. Next, Master Curves were constructed based on the obtained results, following the TTSP method, shifting the G* and δ values with respect to the reference temperature of 25ºC. Figure 5-2 (a) shows the results for the unaged binders, in which the highest G* was noted for 4% OMMT 1 and 4% OMMT 2, followed by 2% OMMT 1 and OMMT 2 throughout all frequencies. The master curves for the RTFO-aged binder are shown in Figure 5-2 (b). As can be seen, under low frequencies such as 0.01 rad/s, the neat binder presents the lowest G*, followed by the binders with 2% nanoclay, then 4% nanoclays. Both 4% OMMT 1 and 4% OMMT 2 demonstrated very similar behaviour at short-term ageing conditions, with the highest G* and enhanced rutting resistance.

Figure 5-2 (c) shows the asphalt binders' G* master curves at 25°C under PAV-aged conditions. At high frequencies, representative of the low-temperature cracking resistance of the binder, 4% OMMT 1 and 2 showed higher G*in comparison to the other samples. However, the differences between the G* at 100 rad/s reduced angular frequency for all five binders

seem insignificant. These results also confirm the BBR performance tests, as shown in Table 5-2.

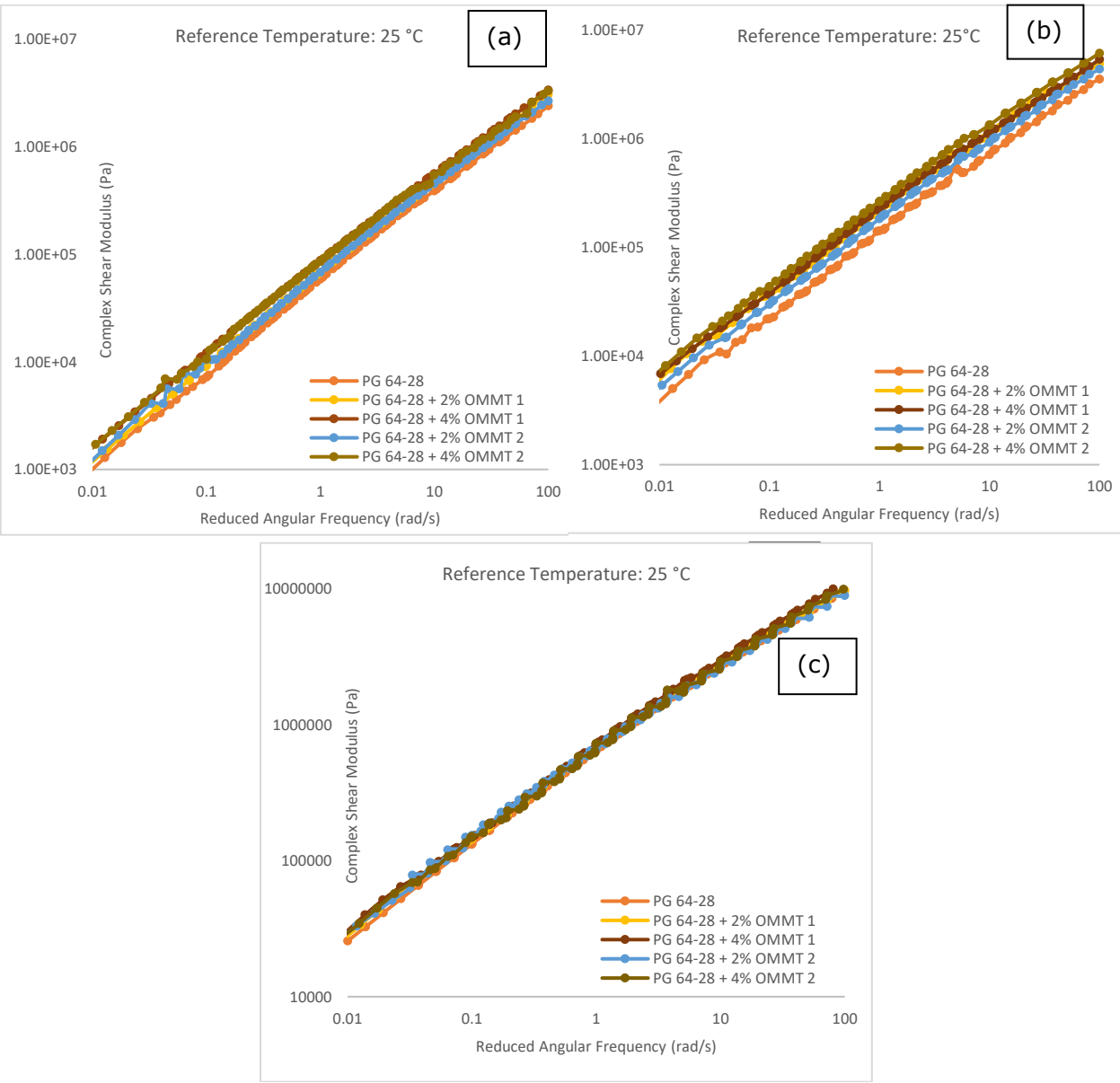

Figure 5-2. Asphalt binders G* Master Curves at 25°C for samples: (a) Unaged, (b) RTFO-aged, (c) PAV-aged

Additionally, δ master curves were constructed at 25°C as shown in Figure 5-3. The study of the δ parameter is also critical as it indicates the viscoelastic behaviour of the binder, as lower phase angle equal to more elastic behaviour. Unlike the G*, the trend difference seems constant irrespective of frequencies. Figure 5-3 (a) shows the results for the unaged samples,

where it is seen that under any reduced angular frequency, the δ for the binders are ranked from highest to lowest in the following order: neat, 2% OMMT 2, 2% OMMT 1, 4% OMMT 1 and 4% OMMT 2. The δ master curves for RTFO-aged samples, which are suitable for characterization of the rutting parameter of asphalts, are shown in Figure 5-3 (b). At low Frequency, OMMT 1 and OMMT 2 behaved very similarly. The samples with 4% nanoclays have better rutting parameters than the ones with 2% nanoclays, by which themselves act better than the neat binder. Under PAV-aged conditions, an analysis under high frequencies best fits the asphalt demands. The δ for all binders behave very similarly under 100 rad/s reduced angular frequency, such as that comparing the five samples, the 4% OMMT 1 has the highest δ, while the 4% OMMT 2 has the lowest, as shown in Figure 5-3 (c).

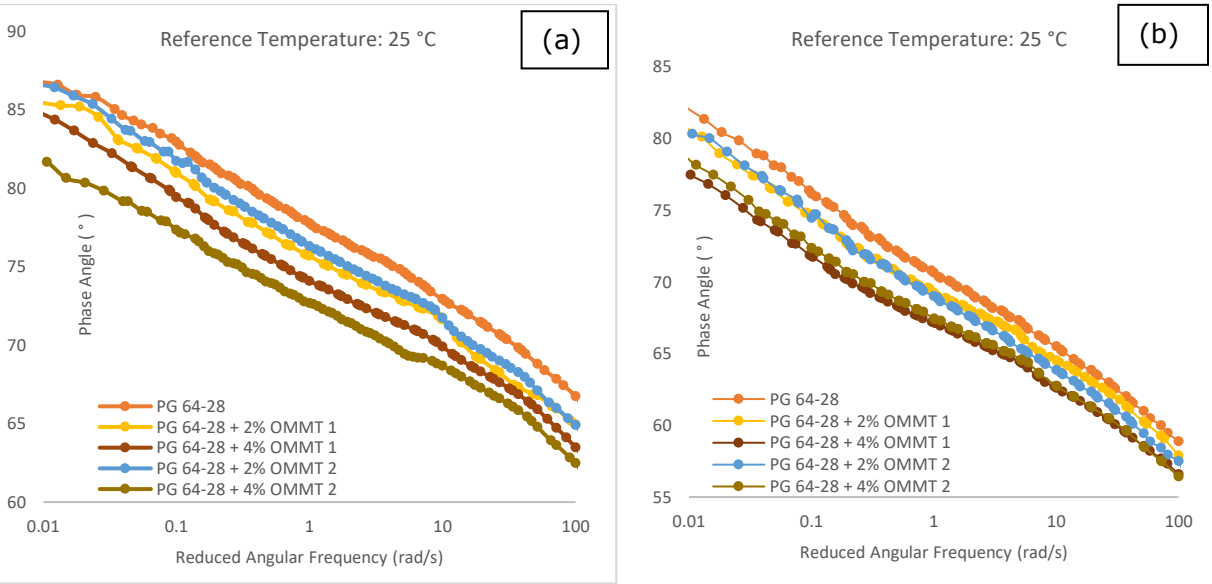

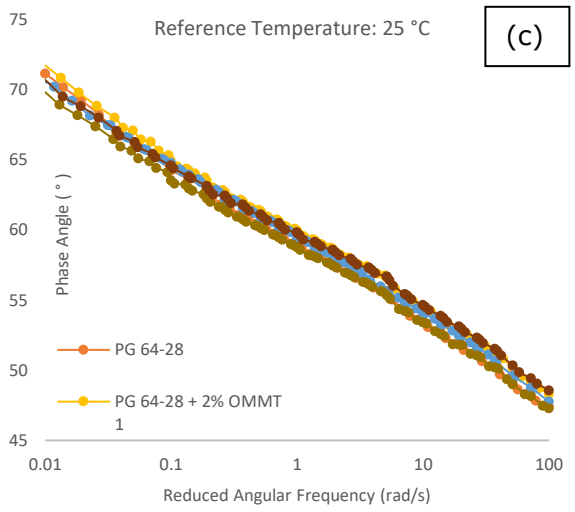

Figure 5-3. Asphalt binders δ Master Curves at 25°C for samples: (a) Unaged, (b) RTFO-aged, (c) PAV-aged

Finally, to confirm nanoclay modification's impact on the modified binders' short-term ageing susceptibility, the FS results were used to calculate the Superpave rutting parameter (G*/sin(δ)). Higher G*/sin(δ) values, as shown in Figure 5-4, indicate higher resistance to rutting, thus from the figure analysis, improvements in this parameter are seen by nanoclay modification. Both unaged and RTFO-aged binders were had the following increasing order for rutting resistance: neat binder, 2% OMMT 1 or 2% OMMT 2, and 4% OMMT 1 or 4% OMMT 2. It is worth mentioning that the obtained results are aligned with the performance grade improvements provided in Table 5-2 for nanoclay modified binders for both unconditioned and short-term aged binders.

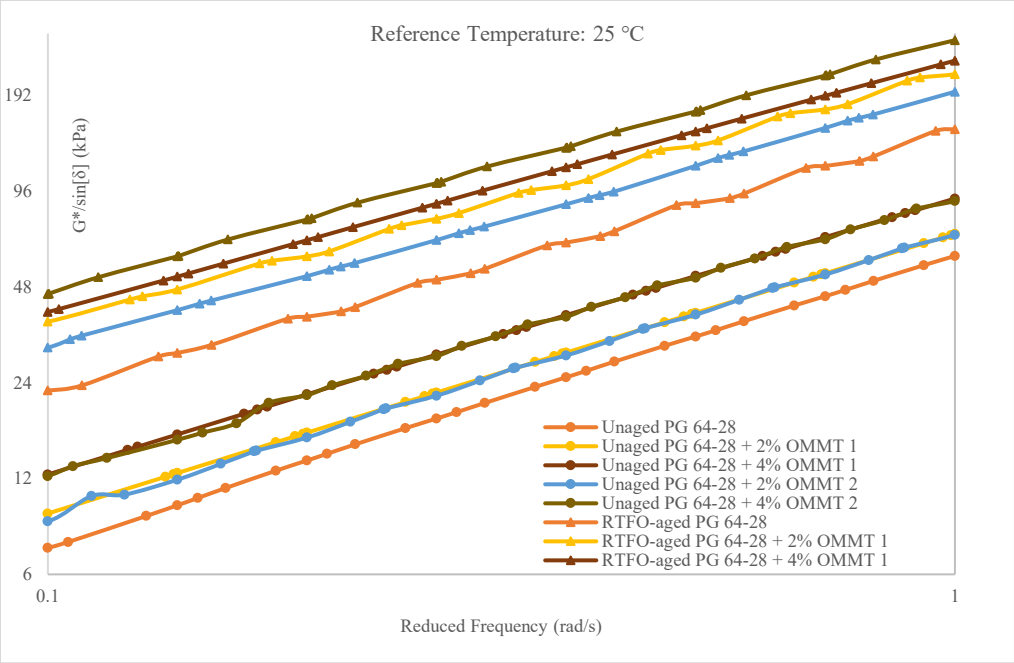

Figure 5-4. Rutting parameter for the unmodified and nanoclay modified asphalt binders

5.4.4 Ageing Indices

For further analysis, the ageing indices of CAI and PAI were calculated accordingly. Figure 5-5 shows the variation in the CAI, where a higher value represents a more significant effect of the ageing conditioning on the specimens. It is noticeable from Figure 5-5 (a) that the neat binder has a lower impact from RTFO-aging than the nanoclay modified binders. The OMMT 1 modified binders had higher CAI from RTFO-aging than those modified with OMMT 2, which agrees with the SARA results, as the OMMT 1 increased the fraction of aromatics, while OMMT 2 decreased it. Long-term ageing effects are significant at high and medium frequencies due to fatigue and low-temperature cracking impacts. Figure 5-5 (b) shows the CAI values for the PAV-aged binders. It could be observed that the modified binders, regardless of the OMMT concentration, have lower CAI values at higher loading frequencies compared to the neat binder. The binders with 4% nanoclays had the lowest CAI values at mid-frequencies, followed by the binders with 2% OMMT concentration and the neat binder.

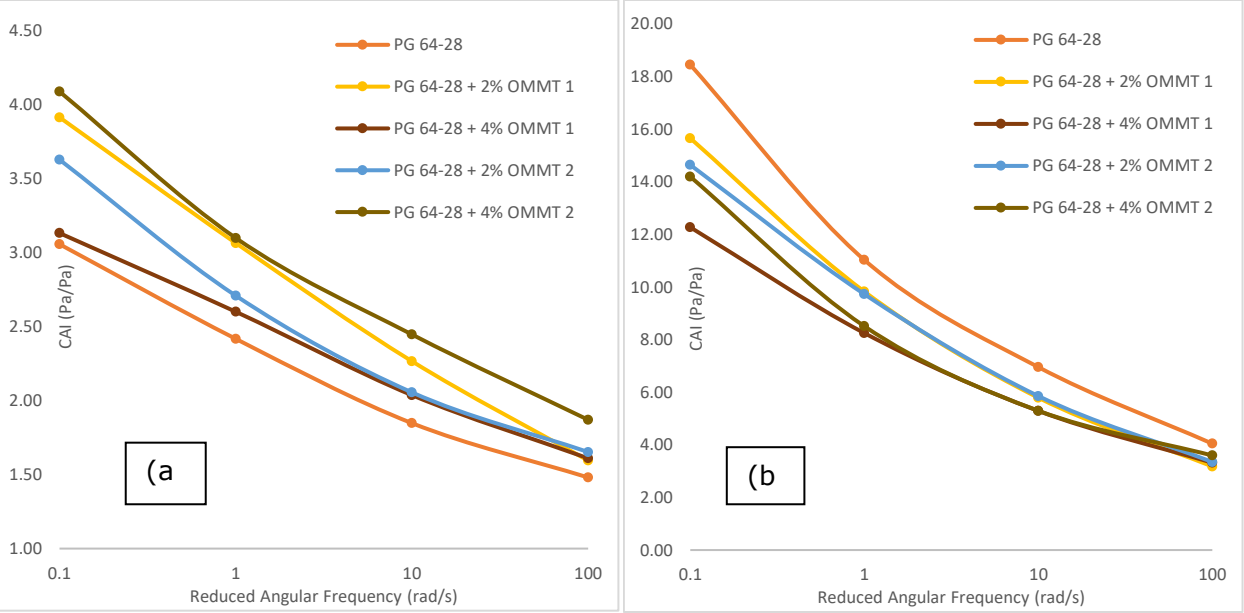

Figure 5-5. CAI graphs for samples: (a) RTFO-aged, (b) PAV-aged

Asphalt binders resist ageing better when the ageing index PAI is higher. FS results were used to calculate the PAI values for short-term and long-term aged asphalt, as presented in Figure 5-6. According to Figure 5-6 (a), the 4% OMMT 2 modified binder behaves better after RTFO ageing than the other samples, indicating the binder is more resistant to short-term ageing. The PAI for PAV-aged binders are illustrated in Figure 5-6 (b). As can be seen from this figure, overall, the PAI increases in the following order: neat binder, 2% OMMT 2, 2% OMMT 1, 4% OMMT 2, and 4% OMMT 1. This order indicates that nanoclay modified asphalt binders are more resistant to long-term ageing and improve at higher concentrations of nanoclays.

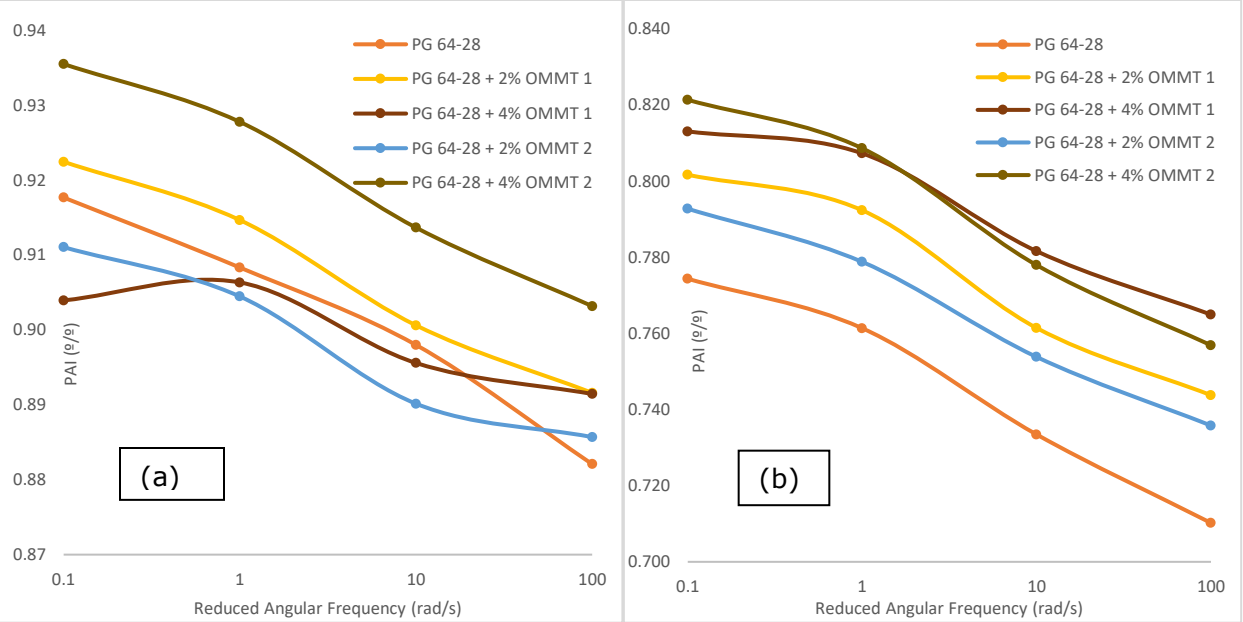

Figure 5-6. PAI graphs for samples: (a) RTFO-aged, (b) PAV-aged

Based on the results, both OMMT 1 and OMMT 2 reduced the impact of long-term ageing under mid and high frequencies, which agrees with the hypothesis that nanoclay silicates block oxidation [16].

5.5 Conclusions

The impact of nanoclay (OMMT) modification on the chemical (SARA fractions) and rheological properties of the asphalt binder was investigated. In addition, the ageing behaviour of the asphalt binder before and after OMMT modification was studied in this research. Based on the obtained results, the following conclusions can be derived:

- The 4% OMMT 1 and 4% OMMT 2 modified asphalt binder showed to be very stable with the CI values of 0.76 and 0.81, respectively, compared to 0.88 for the non-modified binder
- The high-temperature PG grades were increased to 70 for the binders modified with 4% OMMT 1 and 4% OMMT 2, while the PG grade for the neat asphalt binder was 64-28.

- Under 0.01 rad/s angular frequency, among the RTFO-aged samples, the neat binder had the lowest complex shear modulus (G*), followed by the binders modified with 2% and 4% nanoclays.
- The differences between the G* values at higher frequencies (e.g., 100 rad/s) for all five PAV-aged binders seemed insignificant.
- Phase angle (δ) master curves demonstrated that both OMMT 1 and OMMT 2 modified asphalt binders behaved similarly at lower frequencies after short-term (RTFO) ageing.
- According to CAI and PAI analysis, the rutting resistances were improved at lower frequencies after nanoclay modifications. Also, the impact of ageing on the binders was reduced due to the modifications.
- The performance grading results, rheological parameters (G* and δ), and the ageing indices of CAI and PAI were in conformance with each other.

6 Summary and Conclusions

Nanoclays for pavement applications is a trending technology with high potential to improve the rheological, mechanical, and healing properties of asphalt binders, mixtures, and pavement. Consequently, laboratory investigations were conducted on nanoclay modified binder and mix to obtain results about field applicability. Two types of nanoclays, Cloisite 15A (OMMT 1) and Cloisite 20A (OMMT 2), were dispersed into an asphalt binder and investigated under molecular composition Superpave tests and non-standardized behaviour analysis tests.

The main conclusions drawn from the study are summarized as follows:

- The Scanning Electron Microscope images showed that the method used in this study for mixing surface-modified montmorillonites, by employing a High Shear Mixer under 3,000 RPM at 130°C, provides a good dispersion of the material in the matrix.
- The Superpave performance grade results for nanoclay modified asphalt binders indicated that the addition of montmorillonites increases the high-temperature rutting performance of asphalt binders without degrading the low-temperature cracking resistance. The PG grade rises according to the concentration of nanoclay, 5.8 increase for both 4% of Cloisite 15A and 4% Cloisite 20A compared to the neat binder.
- At a binder level, the nanoclay-modification improved the intrinsic healing of asphalt binders. Initial strength gain was the most improved parameter of nanoclay modified binders. Initial strength regained 12.3% to 19.8% higher for 2% weight of nanoclays and 32% to 37.6% higher for 4% concentration nanoclays compared to the neat binder.
- Following a full crack in asphalt surfaces, the intrinsic healing of asphalt binders is vastly improved with the near full-strength regain. The binders modified with 4% Cloisite 15A and 4% Cloisite 20A recovered 96% and 93%, respectively, compared to 79% for the neat binder.

- Nanoclay modification increased the complex shear modulus (G*) of asphalt binders for neat and recovered asphalt binders, with more values for healed binders. G* ratio of modified with 4% Cloisite 15 A to neat binders was 1.88.
- SARA fractions were used to analyze the binders. Nanoclay-modification provided storage stables asphalt binders with Colloidal Index (CI) values below 0.9, as expected for stability. The 4% Cloisite 15A and 4% Cloisite 20A exhibited CI values of 0.76 and 0.81, respectively, compared to 0.88 for the neat binder.
- Using the frequency-sweep test results and master curves, at 0.01 rad/s angular frequency, RTFO-aged samples indicated that G* increases with concentrations of nanoclays in the following order: neat binder, 2% nanoclay following 4% nanoclay-modified binders.
- At high frequencies, which indicate lower temperature behaviour, the differences in G* and phase angle (δ) between all PAV-aged binders seemed insignificant.
- Ageing indices CAI and PAI indicated that for RTFO-aged binders, the rutting resistance was improved by nanoclay modification, aligning with the results observed from the Superpave rutting parameter.
- Finally, the CAI and PAI results indicated a higher long-term ageing resistance of asphalt binder modified by 4% nanoclays.

References

1. Mallick RB, El-Korchi T. Pavement Engineering: Principles and Practice. 1st ed. New York: CRC Pres; 2008.

2. de Rooij M, Van Tittelboom K, De Belie N, Schlangen E, editors. Self-Healing Phenomena in Cement-Based Materials [Internet]. Dordrecht: Springer Netherlands; 2013 [cited 2020 Dec 29]. (RILEM State-of-the-Art Reports; vol. 11). Available from: http://link.springer.com/10.1007/978-94-007-6624-2

3. Little DN, Lytton RL, Williams D, Chen CW. Microdamage healing in asphalt and asphalt concrete, Volume 1 : microdamage and microdamage healing, project summary report. College Station: Texas Transportation Institute; 2001 Jun p. 88. Report No.: FHWA-RD-98-141.

4. Xu S, García A, Su J, Liu Q, Tabaković A, Schlangen E. Self-Healing Asphalt Review: From Idea to Practice. Adv Mater Interfaces. 2018 Sep;5(17):1800536.

5. Bhasin A, Little DN, Bommavaram R, Vasconcelos K. A Framework to Quantify the Effect of Healing in Bituminous Materials using Material Properties. Road Mater Pavement Des. 2008 Jan;9(sup1):219–42.

6. Qiu J. Self Healing of Asphalt Mixtures - Towards a Better Understanding of the Mechanism. [Delft]: Delft University of Technology; 2012.

7. Lv Q, Huang W, Xiao F. Laboratory evaluation of self-healing properties of various modified asphalt. Constr Build Mater. 2017 Apr;136:192–201.

8. Santagata E, Baglieri O, Dalmazzo D, Tsantilis L. Rheological and chemical investigation on the damage and healing properties of bituminous binders. Asph Paving Technol Assoc Asph Paving Technol-Proc Tech Sess. 2009 Jan 1;78:567–95.

9. Huang W, Lv Q, Xiao F. Investigation of using binder bond strength test to evaluate adhesion and self-healing properties of modified asphalt binders. Constr Build Mater. 2016 Jun;113:49–56.

10. Zhou L, Huang W, Zhang Y, Lv Q, Yan C, Jiao Y. Evaluation of the adhesion and healing properties of modified asphalt binders. Constr Build Mater. 2020 Aug;251:119026.

11. Hossain Z, Zaman M, Saha MC, Hawa T. Evaluation of Moisture Susceptibility and Healing Properties of Nanoclay-Modified Asphalt Binders. In: IFCEE 2015 [Internet]. San Antonio, Texas: American Society of Civil Engineers; 2015 [cited 2020 Dec 29]. p. 339–48. Available from: http://ascelibrary.org/doi/10.1061/9780784479087.034

12. Galooyak SS, Dabir B, Nazarbeygi AE, Moeini A. Rheological properties and storage stability of bitumen/SBS/montmorillonite composites. Constr Build Mater. 2010 Mar;24(3):300–7.

13. Hao G, Huang W, Yuan J, Tang N, Xiao F. Effect of aging on chemical and rheological properties of SBS modified asphalt with different compositions. Constr Build Mater. 2017 Dec;156:902–10.

14. Uddin F. Clays, Nanoclays, and Montmorillonite Minerals. Metall Mater Trans A. 2008 Dec;39(12):2804–14.

15. Gilman JW. Flammability and thermal stability studies of polymer layered-silicate žclay/ nanocomposites. 1999;19.

16. Yu J-Y, Feng P-C, Zhang H-L, Wu S-P. Effect of organo-montmorillonite on aging properties of asphalt. Constr Build Mater. 2009 Jul;23(7):2636–40.

17. Krishnan JM, Rajagopal KR. On the mechanical behavior of asphalt. Mech Mater. 2005 Nov;37(11):1085–100.

18. Povolo F, Fontelos M. Time-temperature superposition principle and scaling behaviour. J Mater Sci. 1987 May;22(5):1530–4.

19. Hunter RN, Self A, Read J. The Shell Bitumen handbook. Sixth edition. Westminster, London: Published for Shell Bitumen by ICE Publishing; 2015. 788 p.

20. Cominsky RJ, National Research Council. The superpave mix manual for new construction and overlays /Ronald J. Cominsky. Washington, DC; 1994. 172 p. (Strategic Highway Research Program, SHRP-A).

21. AASHTO T 240-13. Effect of Heat and Air on a Moving Film of Asphalt Binder (Rolling Thin-Film Oven Test). Washington, D.C: American Association of State Highway and Transportation Officials; 2017. (AASHTO provisional standards).

22. AASHTO R 28-12. Accelerated Aging of Asphalt Binder Using a Pressurized Aging Vessel (PAV). Washington, D.C: American Association of State Highway and Transportation Officials; 2018. (AASHTO provisional standards).

23. R 29-15 - Grading or Verifying the Performance Grade (PG) of an Asphalt Binder. 2018;6.

24. AASHTO T 315-20. Determining the Rheological Properties of Asphalt Binder Using a Dynamic Shear Rheometer (DSR). Washington, D.C: American Association of State Highway and Transportation Officials; 2020. (AASHTO provisional standards).

25. AASHTO M 320. Performance-Graded Asphalt Binder. Washington, D.C: American Association of State Highway and Transportation Officials; 2017. (AASHTO provisional standards).

26. AASHTO T 313-12. Determinning the Flexural Creep Stiffness of Asphalt Binder Using the Bending Beam Rheometer (BBR). Washington, D.C: American Association of State Highway and Transportation Officials; 2016. (AASHTO provisional standards).

27. AASHTO T 316-13. Viscosity Determination of Asphalt Binder Using Rotational Viscometer. Washington, D.C: American Association of State Highway and Transportation Officials; 2017. (AASHTO provisional standards).

28. Watson DE, West RC, Turner PA, Casola JR, Transportation Research Board, National Cooperative Highway Research Program, et al. Mixing and Compaction Temperatures of Asphalt Binders in Hot-Mix Asphalt [Internet]. Washington, D.C.: National Academies Press; 2010 [cited 2022 Jan 3]. Available from: http://www.nap.edu/catalog/14367

29. Yildirim Y, Ideker J, Hazlett D. Evaluation of Viscosity Values for Mixing and Compaction Temperatures. J Mater Civ Eng. 2006 Aug;18(4):545–53.

30. Anjan Kumar S, Sarvanan U, Murali Krishnan J, Veeraragavan A. Rheological characterisation of modified binders at mixing and compaction temperature. Int J Pavement Eng. 2014 Oct 21;15(9):767–85.

31. Azimi Alamdary Y, Baaj H. Time–temperature superposition of asphalt materials and temperature sensitivity of rheological parameters (TSRP). Can J Civ Eng. 2021 Oct;48(10):1354–63.

32. Gao J, Wang H, You Z, Mohd Hasan MR. Research on properties of bio-asphalt binders based on time and frequency sweep test. Constr Build Mater. 2018 Jan;160:786–93.

33. AASHTO T 166-16. Bulk Specific Gravity (Gmb) of Compacted Asphalt Mixtures Using Saturated Surface-Dry Specimens. Washington, D.C.: American Association of State Highway and Transportation Officials; 2016. (AASHTO provisional standards).

34. AASHTO T 209-12. Theoretical Maximum Specific Gravity (Gmm) and Density of Hot Mix Asphalt. Washington, D.C: American Association of State Highway and Transportation Officials; 2016. (AASHTO provisional standards).

35. AASHTO T 378-17. Determining the Dynamic Modulus and Flow Number for Asphalt Mixtures Using the Asphalt Mixture Performance Tester (AMPT). Washington, D.C: American Association of State Highway and Transportation Officials; 2017. (AASHTO provisional standards).

36. AASHTO R 87-18. Determining Pavement Deformation Parameters and Cross Slope from Collected Transverse Profiles. Washington, D.C: American Association of State Highway and Transportation Officials; 2018 p. 7. (AASHTO provisional standards).

37. AASHTO T 321-17. Determining the Fatigue Life of Compacted Asphalt Mixtures Subjected to Repeated Flexural Bending. Washington, D.C.: American Association of State Highway and Transportation Officials; 2017. (AASHTO provisional standards).

38. Zwaag S van der, editor. Self healing materials: an alternative approach to 20 centuries of materials science. Dordrecht: Springer; 2007. 385 p. (Springer series in materials science).

39. Blaiszik BJ, Kramer SLB, Olugebefola SC, Moore JS, Sottos NR, White SR. Self-Healing Polymers and Composites. Annu Rev Mater Res. 2010 Jun;40(1):179–211.

40. Kosarli M, Bekas D, Tsirka K, Paipetis AS. Capsule-based self-healing polymers and composites. In: Self-Healing Polymer-Based Systems [Internet]. Elsevier; 2020 [cited 2020 Dec 29]. p. 259–78. Available from: https://linkinghub.elsevier.com/retrieve/pii/B9780128184509000106

41. White SR, Sottos NR, Geubelle PH, Moore JS, Kessler MR, Sriram SR, et al. Autonomic healing of polymer composites. Nature. 2001 Feb 15;409(6822):794–7.

42. Lee MW, An S, Yoon SS, Yarin AL. Advances in self-healing materials based on vascular networks with mechanical self-repair characteristics. Adv Colloid Interface Sci. 2018 Feb 1;252:21–37.

43. Zhang X-L, Su J-F, Guo Y-D, Wang X-Y, Fang Y, Ding Z, et al. Novel vascular self-nourishing and self-healing hollow fibers containing oily rejuvenator for bitumen. Constr Build Mater. 2018 Sep;183:150–62.

44. Wool RP, O'Connor KM. Time dependence of crack healing. J Polym Sci Polym Lett Ed. 1982 Jan;20(1):7–16.

45. Liang B, Lan F, Shi K, Qian G, Liu Z, Zheng J. Review on the self-healing of asphalt materials: Mechanism, affecting factors, assessments and improvements. Constr Build Mater. 2021 Jan;266:120453.

46. Little DN, Bhasin A. Exploring Mechanism of H ealing in Asphalt Mixtures and Quantifying its Impact. In: Springer Series in Materials Science [Internet]. Springer Netherlands; 2007. p. 205–18. Available from: https://dx.doi.org/10.1007/978-1-4020-6250-6_10

47. Tang J, Liu Q, Wu S, Ye Q, Sun Y, Schlangen E. Investigation of the optimal self-healing temperatures and healing time of asphalt binders. Constr Build Mater. 2016;113:1029–33.

48. Sun D, Yu F, Li L, Lin T, Zhu XY. Effect of chemical composition and structure of asphalt binders on self-healing. Constr Build Mater. 2017;133:495–501.

49. Bommavaram RR, Bhasin A, Little DN. Determining Intrinsic Healing Properties of Asphalt Binders: Role of Dynamic Shear Rheometer. Transp Res Rec J Transp Res Board. 2009 Jan;2126(1):47–54.

50. Cheng D, Little DN, Lytton RL, Holste JC. Surface Energy Measurement of Asphalt and Its Application to Predicting Fatigue and Healing in Asphalt Mixtures. Transp Res Rec J Transp Res Board. 2002 Jan;1810(1):44–53.

51. Daniel JS, Kim YR. Laboratory Evaluation of Fatigue Damage and Healing of Asphalt Mixtures. J Mater Civ Eng. 2001 Dec;13(6):434–40.

52. Anderson SD, Fisher DJ. Constructibility review process for transportation facilities. Washington, D.C: National Academy Press; 1997. 88 p. (Report / National Cooperative Highway Research Program).

53. Prager S, Tirrell M. The healing process at polymer–polymer interfaces. J Chem Phys. 1981 Nov 15;75(10):5194–8.

54. Sun D, Sun G, Zhu X, Ye F, Xu J. Intrinsic temperature sensitive self-healing character of asphalt binders based on molecular dynamics simulations. Fuel. 2018;211:609–20.

55. Vo HV, Park D-W, Seo J-W, Le THM. Effects of asphalt types and aging on healing performance of asphalt mixtures using induction heating method. J Traffic Transp Eng Engl Ed. 2020;7(2):227–36.

56. Tabaković A, Schlangen E. Self-Healing Technology for Asphalt Pavements. In: Hager MD, van der Zwaag S, Schubert US, editors. Self-healing Materials [Internet]. Cham: Springer International Publishing; 2015 [cited 2020 Dec 29]. p. 285–306. (Advances in Polymer Science; vol. 273). Available from: http://link.springer.com/10.1007/12_2015_335

57. Xiang H, Zhang W, Liu P, He Z. Fatigue–healing performance evaluation of asphalt mixture using four-point bending test. Mater Struct. 2020 Jun;53(3):47.

58. Rooholamini H, Imaninasab R, Vamegh M. Experimental analysis of the influence of SBS/nanoclay addition on asphalt fatigue and thermal performance. Int J Pavement Eng. 2019 Jun 3;20(6):628–37.

59. Bergaya F, Lagaly G. Chapter 1 General Introduction: Clays, Clay Minerals, and Clay Science. In: Developments in Clay Science [Internet]. Elsevier; 2006. p. 1–18. Available from: https://dx.doi.org/10.1016/s1572-4352(05)01001-9

60. Jahromi SG, Andalibizade B, Vossough S. Engineering properties of nanoclay modified asphalt concrete mixtures. Arabian Journal for Science & Engineering. 2010;16.

61. Kaufhold S, Dohrmann R, Ufer K, Meyer FM. Comparison of methods for the quantification of montmorillonite in bentonites. Appl Clay Sci. 2002;22(3):145–51.

62. Lan T, Kaviratna PD, Pinnavaia TJ. Mechanism of Clay Tactoid Exfoliation in Epoxy-Clay Nanocomposites. Chem Mater. 1995;7(11):2144–50.

63. Ghile DB. Effect of nanoclay modification on rheology of bitumen and on performance of asphalt mixtures. [Delf]: Delf University; 2006.

64. Xu X, Liu F, Jiang L, Zhu JY, Haagenson D, Wiesenborn DP. Cellulose Nanocrystals vs. Cellulose Nanofibrils: A Comparative Study on Their Microstructures and Effects as Polymer Reinforcing Agents. ACS Appl Mater Interfaces. 2013;5(8):2999–3009.

65. Ezzat H, El-Badawy S, Gabr A, Zaki E-SI, Breakah T. Evaluation of Asphalt Binders Modified with Nanoclay and Nanosilica. Procedia Eng. 2016;143:1260–7.

66. Ameri M, Nobakht S, Bemana K, Vamegh M, Rooholamini H. Effects of nanoclay on hot mix asphalt performance. Pet Sci Technol. 2016 Apr 17;34(8):747–53.

67. Bagshaw SA, Kemmitt T, Waterland M, Brooke S. Effect of blending conditions on nano-clay bitumen nanocomposite properties. Road Mater Pavement Des. 2019 Nov 17;20(8):1735–56.

68. Hossain Z, Zaman M, Saha MC, Hawa T. Evaluation of Viscosity and Rutting Properties of Nanoclay-Modified Asphalt Binders. In: Geo-Congress 2014 Technical Papers [Internet]. Atlanta, Georgia: American Society of Civil Engineers; 2014 [cited 2021 Nov 1]. p. 3695–702. Available from: http://ascelibrary.org/doi/10.1061/9780784413272.358

69. Yu J, Zeng X, Wu S, Wang L, Liu G. Preparation and properties of montmorillonite modified asphalts. Mater Sci Eng A. 2007 Feb;447(1–2):233–8.

70. You Z, Mills-Beale J, Foley JM, Roy S, Odegard GM, Dai Q, et al. Nanoclay-modified asphalt materials: Preparation and characterization. Constr Build Mater. 2011 Feb;25(2):1072–8.

71. Abdullah ME, Zamhari KA, Buhari R, Nayan MN, Mohd Rosli H. Short Term and Long Term Aging Effects of Asphalt Binder Modified with Montmorillonite. Key Eng Mater. 2013 Dec;594–595:996–1002.

72. Zhang H, Yu J, Wang H, Xue L. Investigation of microstructures and ultraviolet aging properties of organo-montmorillonite/SBS modified bitumen. Mater Chem Phys. 2011 Oct;129(3):769–76.

73. Yu R, Fang C, Liu P, Liu X, Li Y. Storage stability and rheological properties of asphalt modified with waste packaging polyethylene and organic montmorillonite. Appl Clay Sci. 2015 Feb;104:1–7.

74. Tian X, Zhang R, Yang Z, Chu Y, Xu Y, Zhang Q. Multiscale Study on the Effect of Nano-Organic Montmorillonite on the Performance of Rubber Asphalt. J Nanomater. 2018 Sep 17;2018:1–10.

75. Wang R, Qi Z, Li R, Yue J. Investigation of the effect of aging on the thermodynamic parameters and the intrinsic healing capability of graphene oxide modified asphalt binders. Constr Build Mater. 2020 Jan;230:116984.

76. Shen S, Chiu H-M, Huang H. Characterization of Fatigue and Healing in Asphalt Binders. J Mater Civ Eng. 2010 Sep;22(9):846–52.

77. Shu B, Wu S, Dong L, Norambuena-Contreras J, Li Y, Li C, et al. Self-healing capability of asphalt mixture containing polymeric composite fibers under acid and saline-alkali water solutions. J Clean Prod. 2020;268:122387.

78. Amani S, Kavussi A, Karimi MM. Effects of aging level on induced heating-healing properties of asphalt mixes. Constr Build Mater. 2020;263:120105.

79. Fakhri M, Bahmai BB, Javadi S, Sharafi M. An evaluation of the mechanical and self-healing properties of warm mix asphalt containing scrap metal additives. J Clean Prod. 2020;253:119963.

80. Baaj H, Mikhailenko P, Almutairi H, Di Benedetto H. Recovery of asphalt mixture stiffness during fatigue loading rest periods. Constr Build Mater. 2018 Jan;158:591–600.

81. Iskender E. Evaluation of mechanical properties of nano-clay modified asphalt mixtures. Measurement. 2016 Nov;93:359–71.

82. Qiu J, van de Ven MFC, Wu S, Yu J, Molenaar AAA. Investigating the Self Healing Capability of Bituminous Binders. Road Mater Pavement Des. 2009 Jan;10(sup1):81–94.

83. Thomas Weaseh Johnson. Application of Nanomaterials in Asphalt Modification. [Edmonton, AB]: University of Alberta; 2020.

84. Hossain Z, Zaman M, Hawa T, Saha MC. Evaluation of Moisture Susceptibility of Nanoclay-Modified Asphalt Binders through the Surface Science Approach. J Mater Civ Eng. 2015 Oct;27(10):04014261.

85. Tabatabaee N, Shafiee MH. Effect of Organoclay Modified Binders on Fatigue Performance. In: Scarpas A, Kringos N, Al-Qadi I, A. L, editors. 7th RILEM International Conference on Cracking in Pavements [Internet]. Dordrecht: Springer Netherlands; 2012 [cited 2020 Dec 29]. p. 869–78. Available from: http://link.springer.com/10.1007/978-94-007-4566-7_84

86. Urban D, Takamura K, editors. Polymer dispersions and their industrial applications. Weinheim: Wiley-VCH; 2002. 408 p.

87. Ahmed RB, Hossain K. Waste cooking oil as an asphalt rejuvenator: A state-of-the-art review. Constr Build Mater. 2020 Jan;230:116985.

88. Leegwater GA, Scarpas A, Erkens SMJG. The influence of boundary conditions on the healing of bitumen. Road Mater Pavement Des. 2018 Apr 3;19(3):571–80.

89. Little DN, Bhasin A, Darabi MK. Damage healing in asphalt pavements. In: Advances in Asphalt Materials [Internet]. Elsevier; 2015 [cited 2021 Jul 18]. p. 205–42. Available from: https://linkinghub.elsevier.com/retrieve/pii/B9780081002698000076

90. Polacco G, Kříž P, Filippi S, Stastna J, Biondi D, Zanzotto L. Rheological properties of asphalt/SBS/clay blends. Eur Polym J. 2008 Nov;44(11):3512–21.

91. Liu S, Zhou SB, Xu Y. Evaluation of cracking properties of SBS-modified binders containing organic montmorillonite. Constr Build Mater. 2018 Jun;175:196–205.

92. Tang XD, Kong XL, He ZG, Li J. Nano-Montmorillonite/SBS Composite Modified Asphalt: Preparation and Aging Property. Mater Sci Forum. 2011 Jun;688:175–9.

93. Blom J, De Kinder B, Meeusen J, Van den bergh W. The influence of nanoclay on the durability properties of asphalt mixtures for top and base layers. IOP Conf Ser Mater Sci Eng. 2017 Sep;236:012007.

94. Johnson TW, Hashemian L. Laboratory Evaluation of Modified Asphalt Mixes Using Nanomaterial. J Test Eval. 2021 Mar 1;49(2):20190840.

95. BYK Additives. BYK-Cloisite-15A-Nanoclay.pdf [Internet]. Songhan Plastic Technology Co., Ltd; 2021. Available from: http://www.lookpolymers.com/

96. BYK Additives. BYK-Cloisite-20A-Nanoclay.pdf [Internet]. Songhan Plastic Technology Co., Ltd; 2021. Available from: http://www.lookpolymers.com/

97. Zhu TT, Zhou CH, Kabwe FB, Wu QQ, Li CS, Zhang JR. Exfoliation of montmorillonite and related properties of clay/polymer nanocomposites. Appl Clay Sci. 2019 Mar;169:48–66.

98. Qiu J, van de Ven M, Molenaar A. Crack-Healing Investigation in Bituminous Materials. J Mater Civ Eng. 2013 Jul;25(7):864–70.

99. Ameri M, Nobakht S, Bemana K, Rooholamini H, Vamegh M. Effect of nanoclay on fatigue life of hot mix asphalt. Pet Sci Technol. 2016 Jun 17;34(11–12):1021–5.

100. Lu X. Fatigue and healing characteristics of bitumens studied using dynamic shear rheometer. In: Sixth International RILEM Symposium on Performance Testing and Evaluation of Bituminous Materials [Internet]. Zurich, Switzerland: RILEM Publications SARL; 2003 [cited 2021 Jul 18]. p. 408–15. Available from: https://www.rilem.net/boutique/fiche.php?cat=conference&reference=pro028-051

101. Santagata E, Baglieri O, Tsantilis L, Dalmazzo D. Evaluation of self healing properties of bituminous binders taking into account steric hardening effects. Constr Build Mater. 2013 Apr;41:60–7.

102. Sun D, Lin T, Zhu X, Tian Y, Liu F. Indices for self-healing performance assessments based on molecular dynamics simulation of asphalt binders. Comput Mater Sci. 2016 Mar;114:86–93.

103. Bhasin A, Palvadi S, Little DN. Influence of Aging and Temperature on Intrinsic Healing of Asphalt Binders. Transp Res Rec J Transp Res Board. 2011 Jan;2207(1):70–8.

104. Qiu J, van de Ven MFC, Wu SP, Yu JY, Molenaar AAA. Investigating self healing behaviour of pure bitumen using Dynamic Shear Rheometer. Fuel. 2011 Aug;90(8):2710–20.

105. Husky Energy. SDS.Asphalt Cements Non-Modified - Husky Oil Operations Limited (Husky Oil Marketing Company). 2019.

106. Baghaee Moghaddam T, Baaj H. The use of rejuvenating agents in production of recycled hot mix asphalt: A systematic review. Constr Build Mater. 2016 Jul;114:805–16.

107. Tanzi MC, Farè S, Candiani G. Mechanical Properties of Materials. In: Foundations of Biomaterials Engineering [Internet]. Elsevier; 2019 [cited 2021 Dec 9]. p. 105–36. Available from: https://linkinghub.elsevier.com/retrieve/pii/B9780081010341000025

108. Liu F, Zhou Z, Zhang X. Construction of complex shear modulus and phase angle master curves for aging asphalt binders. Int J Pavement Eng. 2020 May 12;1–9.

109. Zhang H, Chen Z, Zhu C, Wei C. An innovative and smart road construction material: thermochromic asphalt binder. In: New Materials in Civil Engineering [Internet]. Elsevier; 2020 [cited 2021 Dec 9]. p. 691–716. Available from: https://linkinghub.elsevier.com/retrieve/pii/B9780128189610000223

110. Johnson TW, Hashemian L, Patra S, Shabani A. Application of Nanoclay Materials in Asphalt Pavements. 2019 TAC-ITS Can Jt Conf. 2019;16.

111. Ghasemirad A, Bala N, Hashemian L. High-Temperature Performance Evaluation of Asphaltenes-Modified Asphalt Binders. Molecules. 2020 Jul 22;25(15):3326.

112. Zhang H, Chen Z, Li L, Zhu C. Evaluation of aging behaviors of asphalt with different thermochromic powders. Constr Build Mater. 2017 Nov;155:1198–205.

113. Fang C, Yu R, Liu S, Li Y. Nanomaterials Applied in Asphalt Modification: A Review. J Mater Sci Technol. 2013 Jul;29(7):589–94.

114. Vargas MA, Moreno L, Montiel R, Manero O, Vázquez H. Effects of montmorillonite (Mt) and two different organo-Mt additives on the performance of asphalt. Appl Clay Sci. 2017 Apr;139:20–7.

115. ASTM D6560-17. Test Method for Determination of Asphaltenes (Heptane Insolubles) in Crude Petroleum and Petroleum Products [Internet]. West Conshohocken, PA: ASTM International; 2017 [cited 2021 Aug 9]. Available from: http://www.astm.org/cgi-bin/resolver.cgi?D6560-17

116. ASTM D2007-19. Standard Test Method for Characteristic Groups in Rubber Extender and Processing Oils and Other Petroleum-Derived Oils by the Clay-Gel Absorption Chromatographic Method [Internet]. West Conshohocken, PA: ASTM International; 2019. Available from: http://www.astm.org/doiLink.cgi?MNL10877M

117. Ashoori S, Sharifi M, Masoumi M, Mohammad Salehi M. The relationship between SARA fractions and crude oil stability. Egypt J Pet. 2017 Mar;26(1):209–13.

118. Xu Y, Zhang E, Shan L. Effect of SARA on Rheological Properties of Asphalt Binders. J Mater Civ Eng. 2019 Jun;31(6):04019086.

119. Jing R, Varveri A, Liu X, Scarpas A, Erkens S. Ageing Behavior of Porous and Dense Asphalt Mixtures in the Field. In: Di Benedetto H, Baaj H, Chailleux E, Tebaldi G, Sauzéat C, Mangiafico S, editors. Proceedings of the RILEM International Symposium on Bituminous Materials [Internet]. Cham: Springer International Publishing; 2022 [cited 2021 Dec 7]. p. 191–8. (RILEM Bookseries; vol. 27). Available from: https://link.springer.com/10.1007/978-3-030-46455-4_24

120. Yin Y, Huang W, Lv J, Ma X, Yan J. Unified Construction of Dynamic Rheological Master Curve of Asphalts and Asphalt Mixtures. Int J Civ Eng. 2018 Sep;16(9):1057–67.

121. Jing R, Varveri A, Liu X, Scarpas A, Erkens S. Rheological, fatigue and relaxation properties of aged bitumen. Int J Pavement Eng. 2020 Jul 2;21(8):1024–33.

122. Yue M, Yue J, Wang R, Xiong Y. Evaluating the fatigue characteristics and healing potential of asphalt binder modified with Sasobit® and polymers using linear amplitude sweep test. Constr Build Mater. 2021 Jun;289:123054.

123. Apeagyei AK. Laboratory evaluation of antioxidants for asphalt binders. Constr Build Mater. 2011 Jan;25(1):47–53.

Appendix A

The Rotational Viscometer (RV) method, used to determine the mixing and compaction temperatures of unmodified asphalt binders, is not appropriate to determine these temperatures for modified samples. The results obtained from RV for modified samples presents values higher than needed for coating the aggregates. The steady shear flow is presents more reliable results for mixing and compaction temperatures. For this reason, the steady shear flow test was employed on all binders used in this work, the graph is presented in Figure A-1, while the mixing and compaction temperatures are presented in Table A-1.

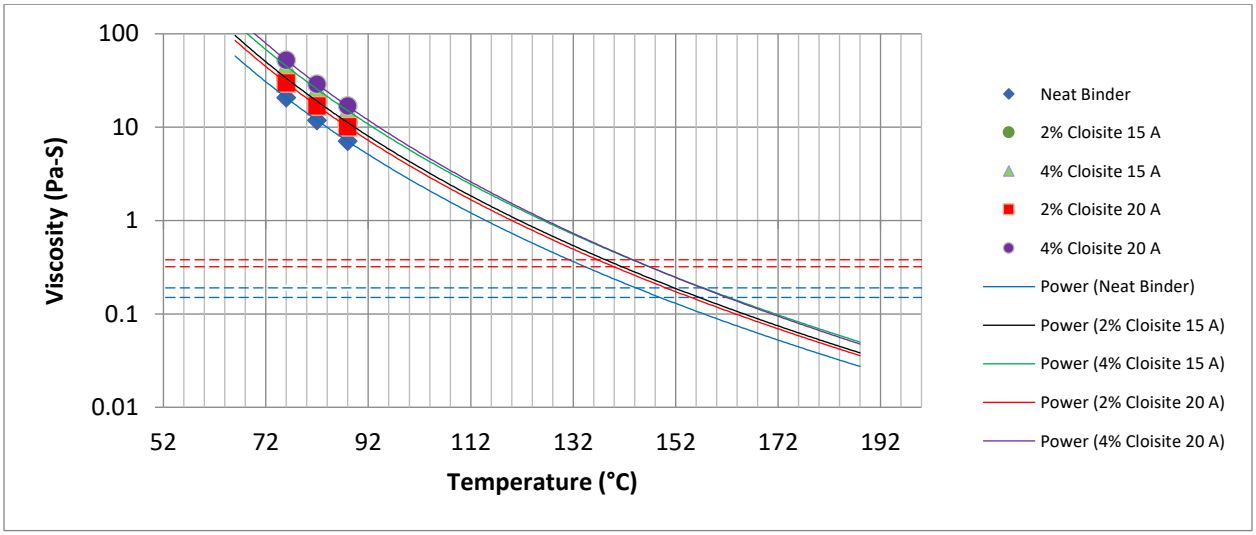

Figure A-1: Steady Shear Flow Mixing and Compaction Curves

Table A-1: Steady Shear Flow Mixing and Compaction Temperatures

Limits	Neat Binder	2% Cloisite 15A	4% Cloisite 15A	2% Cloisite 20A	4% Cloisite 20A
Mixing upper temperature (°C)	149	156	162	155	162
Mixing lower temperature (°C)	144	152	157	150	157
Compaction upper temperature (°C)	133	141	149	140	149
Compaction lower temperature (°C)	129	138	146	137	146

Also, flow and stability of the asphalt mixtures, marshall samples were constructed and tested using a Marshall Stability test equipment, and the results are present in Table A-2.

Table A-2. Flow and Stability results for asphalt mix using 5.5% binder content.

Asphalt binder used	Corrected Flow	Corrected Stability
Neat S1	3.562	14.91
Neat S2	4.161	18.85
Neat S3	3.851	16.17
2% Cloisite 15A S1	3.17	19.95
2% Cloisite 15A S2	3.026	18.34
2% Cloisite 15A S3	3.404	16.81
2% Cloisite 20A S1	3.224	18.05
2% Cloisite 20A S2	3.265	19.08
2% Cloisite 20A S3	3.282	18.63
4% Cloisite 15A S1	3.325	20.29
4% Cloisite 15A S2	3.493	20.38
4% Cloisite 20A S1	3.312	22.38
4% Cloisite 20A S2	2.762	19.48
4% Cloisite 20A S3	3.444	19.90

Appendix B

The asphalt binders modified with nanoclay were investigated using a two-piece healing test, which provided promising results on how it would behave on asphalt pavement. To study this behaviour in a larger scale, a method using a four-point bending test was used. Beams were cut using an electric saw on asphalt slabs as seen on Figure B-1. These beams were subjected to fatigue using as four-point bending test, and then left to heal in an oven at 50 °C, during a specific time (3 hours or 24 hours). After the healing time, the samples were removed from the oven and left in air temperature for rest for 24 hours, then subjected to fatigue again using the four-point bending equipment. All fatigue tests were done in room temperature with 1000 microstrains.

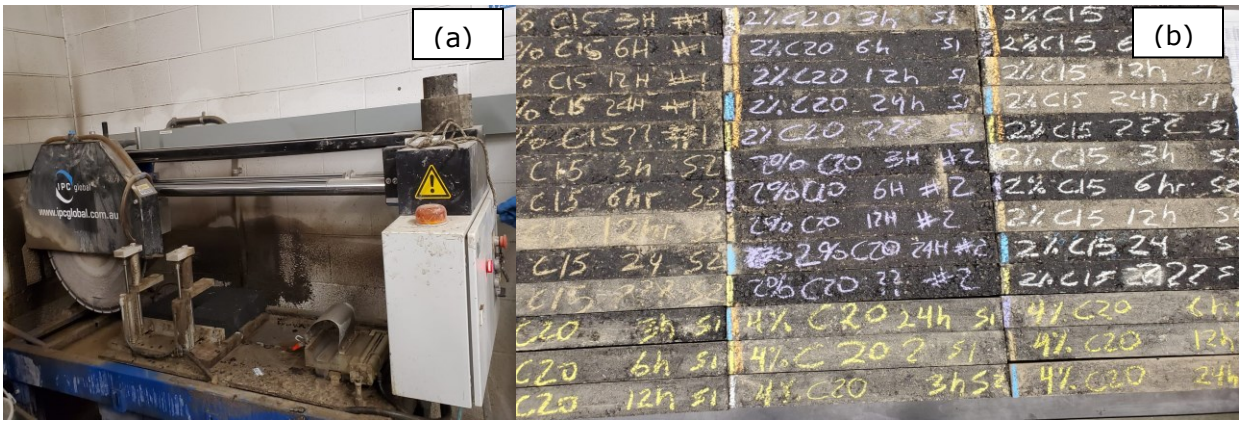

Figure B-1. (a) Electric Saw cutting slab, (b) Asphalt mixture beam of neat and modified binders

The results obtained from the four-point bending test were analyzed by calculating a healing percentage similar to the one used in the two-piece healing test. The fatigue life before healing (N1) was divided by the sum of N1 and fatigue life after healing (N2). The results obtained from these calculations are present in Table B-1 and are similar to the initial healing results obtained from the two-piece healing test.

Table B-1. Healing % of Asphalt mixtures of nanoclay modified asphalt mixtures

Asphalt Mix Sample	H% (N1/(N1+N2))	
	After 3 hours	After 24 hrs
Control	55	58
2% Cloisite 15A	76	71
2% Cloisite 20A	74	71
4% Cloisite 15A	85	90
4% Cloisite 20A	84	76

Appendix C

In order to investigate the properties of nanoclay modified asphalt mixtures, dynamic modulus samples were prepared for neat binder and 4% Cloisite 15A. Superpave samples were compacted, then cored and trimmed. The samples were test in a UTM as seen in Figure C-1.

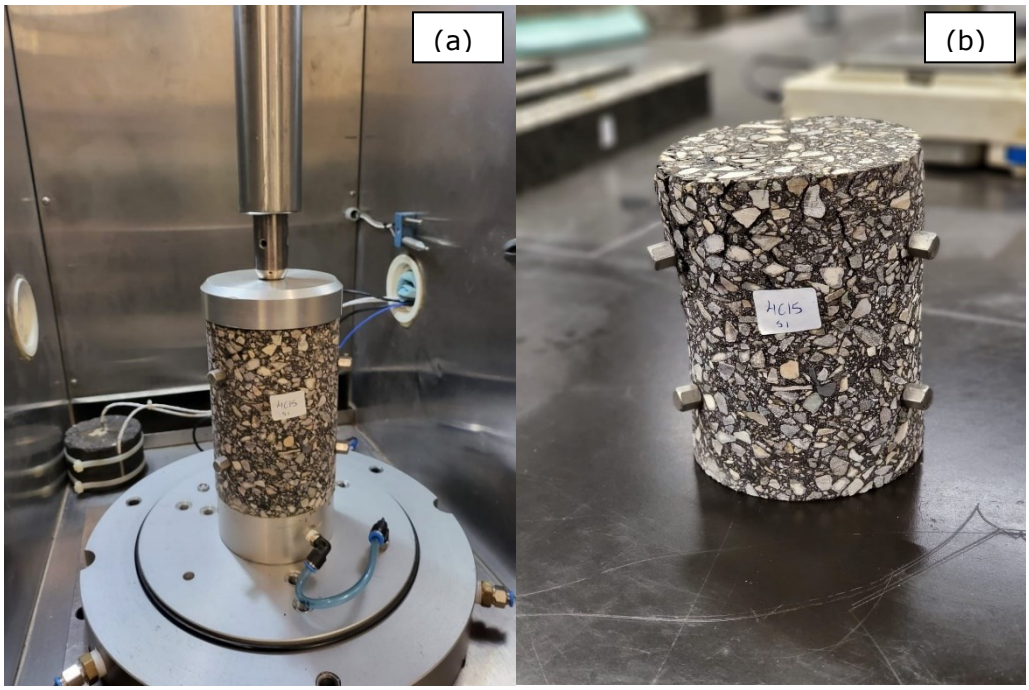

Figure C-1. Dynamic Modulus sample (a) during testing, (b) after testing

The results obtained from the Dynamic Modulus test are presented in Table C-1.

Table C-1. Dynamic Modulus Results

Sample	Parameter	4 °C			20 °C			40 °C			
		10 Hz	1 Hz	0.1 Hz	10 Hz	1 Hz	0.1 Hz	10 Hz	1 Hz	0.1 Hz	0.01 Hz
Neat S1	E* (MPa)	10670	5518	2654	5871	2477	808.1	856.8	247	114.1	78.8
	δ (°)	24.16	31.44	34.88	31.86	35.56	35.07	39.45	34.74	25.76	17.34
Neat S2	E* (MPa)	10155	5115	2423	5212	2064	699.6	839.7	258.8	127.3	86.7
	δ (°)	24.5	32.35	36.45	32.81	36.69	34.24	38.67	32.34	23.35	14.83
4% Cloisite 15A S1	E* (MPa)	14397	8965	5276	7067	3322	1395	1440	501.1	226.7	135.8
	δ (°)	17.93	24.18	28.83	28.06	33.41	33.33	37.88	32.97	26.35	19.39
4% Cloisite 15A S2	E* (MPa)	17896	12031	7274	8608	4274	1857	1514	550.4	259.7	170.4
	δ (°)	14.43	19.65	5.26	26.51	31.28	32.2	36.86	31.96	25.37	18.47